NASA SP-28

STRUCTURES FOR SPACE OPERATIONS

NATIONAL AERONAUTICS AND SPACE ADMINISTRATION • Washington, D.C.
December 1962 • Office of Scientific and Technical Information

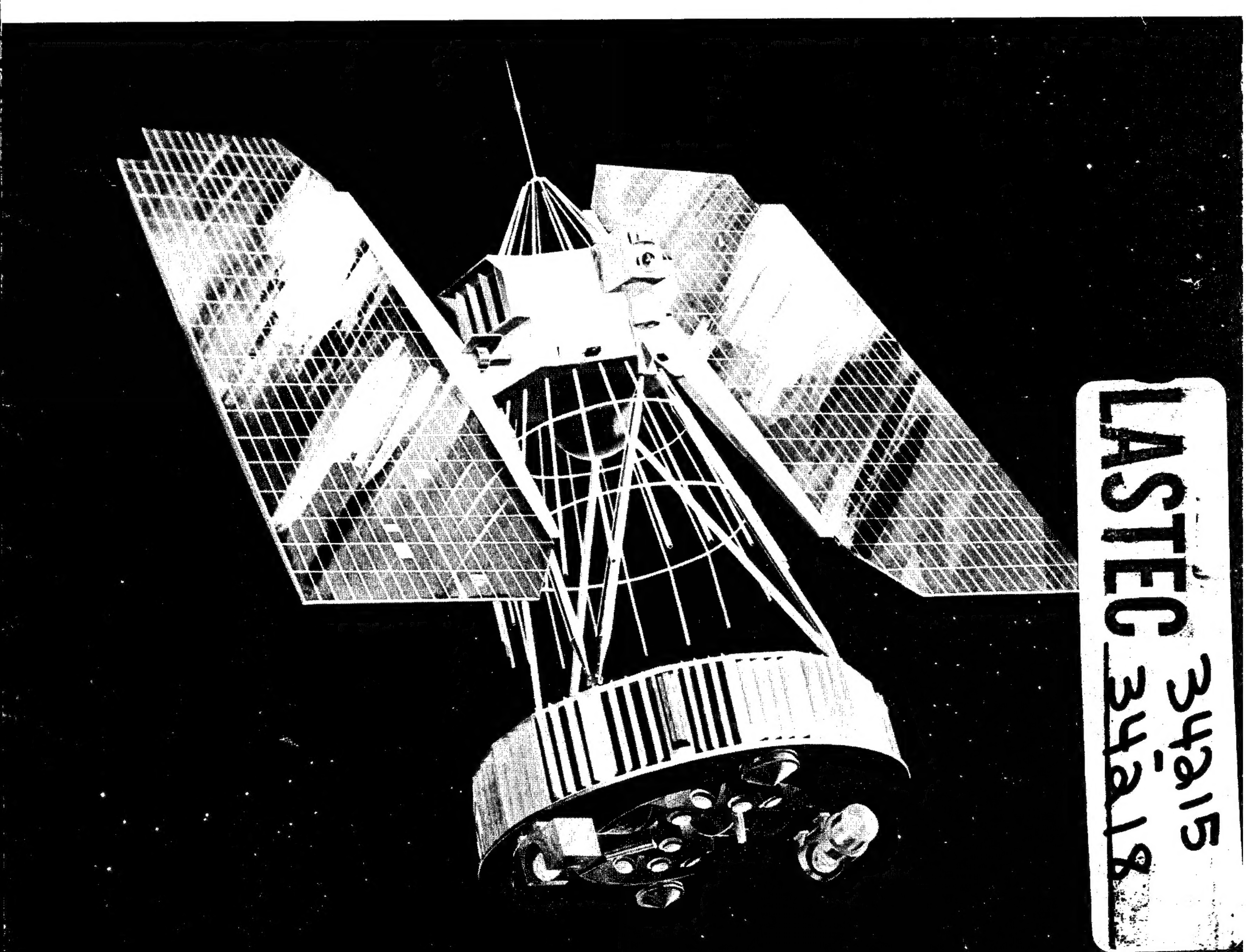

--END ((ENTER NEXT COMMAND)) END --
@str@

*MSG DI4 DROLS PROCESSING - LAST INPUT IGNORED

-- 8 OF 8
-- ***DTIC DOES NOT HAVE THIS ITEM***
-- 1 - AD NUMBER: D428957
-- 5 - CORPORATE AUTHOR: NATIONAL AERONAUTICS AND SPACE ADMINISTRATION
-- WASHINGTON DC
-- 6 - UNCLASSIFIED TITLE: STRUCTURES FOR SPACE OPERATIONS.
--11 - REPORT DATE: NOV 01, 1962
--12 - PAGINATION: 50P
--14 - REPORT NUMBER: NASA SP-28.
--20 - REPORT CLASSIFICATION: UNCLASSIFIED
--21 - SUPPLEMENTARY NOTE: PROCEEDINGS: NASA-UNIVERSITY CONFERENCE ON
-- THE SCIENCE AND TECHNOLOGY OF SPACE EXPLORATION, 'STRUCTURES FOR
-- SPACE OPERATIONS', 1-3 NOV 62, CHICAGO, IL. DEC 62. (SEE PL-34215).
--22 - LIMITATIONS (ALPHA): APPROVED FOR PUBLIC RELEASE; DISTRIBUTION
-- UNLIMITED. [redacted]
--33 - LIMITATION CODES: 1 [redacted]

-- END Y FOR NEXT ACCESSION END

Alt-Z FOR HELP3 ANSI 3 HDX 3 3 LOG CLOSED 3 PRINT OFF 3 PARITY

Add 428957
428960

Foreword

The NASA-University Conference on the Science and Technology of Space Exploration, conducted in Chicago on November 1–3, 1962, was held "to provide an authoritative and up-to-date review of aeronautical and space science technology."

The scientific papers delivered at the conference were grouped for presentation by topics and are, in effect, 1962 state-of-the-art summaries. Accordingly, NASA has published under separate covers sixteen groups of conference papers to make them conveniently available to those interested in specific fields. This series (NASA SP–13 to NASA SP–28) is listed by title and price on the back cover.

All papers presented at the conference have also been published in a two-volume *Proceedings* (NASA SP–11) available from the Superintendent of Documents for $2.50 and $3.00, respectively. Those papers presented herein originally appeared on pages 487 to 532 of Volume 2 of NASA SP–11.

PLASTEC

#

Contents

	Page
RESEARCH, DESIGN CONSIDERATIONS, AND TECHNOLOGICAL PROBLEMS OF STRUCTURES FOR LAUNCH VEHICLES	1
HARRY L. RUNYAN and ROBERT W. LEONARD	
RESEARCH, DESIGN CONSIDERATIONS, AND TECHNOLOGICAL PROBLEMS OF STRUCTURES FOR WINGED AEROSPACE VEHICLES	13
ELDON E. MATHAUSER	
RESEARCH, DESIGN CONSIDERATIONS, AND TECHNOLOGICAL PROBLEMS OF STRUCTURES FOR PLANETARY ENTRY VEHICLES	25
ROGER A. ANDERSON	
RESEARCH, DESIGN CONSIDERATIONS, AND TECHNOLOGICAL PROBLEMS OF STRUCTURES FOR SPACECRAFT	35
GEORGE W. BROOKS	

34216

34217

34218

Research, Design Considerations, and Technological Problems of Structures for Launch Vehicles

By Harry L. Runyan and Robert W. Leonard

HARRY L. RUNYAN, *Head of the Structural Dynamics Branch, Dynamic Loads Division, NASA Langley Research Center, received his Bachelor of Science degree in Mechanical Engineering from Rutgers University in 1939. He joined the Langley staff in December 1945. He was one of the first to obtain his Master of Science degree in Aeronautical Engineering from the University of Virginia through Langley's graduate study program in 1951. Runyan is a renowned authority in the fields of flight loads, structural dynamics, and flutter and vibration of missiles and aircraft. He has achieved national and international recognition for fundamental research in such areas as analytical technique for determining oscillating air forces on a wing of arbitrary planform, flutter at hypersonic speeds, launch vehicle dynamics, and others. He is frequently called upon to present important papers before technical conferences and symposiums. Runyan is an Associate Fellow of the Institute of the Aerospace Sciences, a member of the American Geophysical Union, and a member of the Engineers' Club of the Virginia Peninsula.*

DR. ROBERT W. LEONARD, *Head of the Structural Mechanics Branch, Structures Research Division, NASA Langley Research Center, received his Bachelor of Science degree in Naval Technology from the University of Minnesota in February 1946. He received his Master of Science and Doctorate in Engineering Mechanics from the University of Nebraska and Virginia Polytechnic Institute in 1949 and 1961, respectively. Dr. Leonard joined the Langley staff in August 1949 and has specialized in research on response of continuous structures to transient loads, panel flutter, analysis of expandable structures, and thin shell and membrane theory. He has also undertaken the solution of certain structural problems arising in the development of the Echo II passive communications satellite. Dr. Leonard is currently a member of the Structures Criteria Subcommittee of the NASA Design Criteria Steering Committee of the ASME (serving on Spacecraft and Structures Committee of the Aviation and Space Division), and of Sigma Xi honorary fraternity.*

SUMMARY

Some of the branches of the technology needed in the reliable and efficient design of launch-vehicle structures are discussed. Included are shell buckling, stress analysis, panel flutter, noise, vehicle response to horizontal winds, vibrations, dynamic modeling, and the study of new configuration concepts as complete systems. Examples are shown to indicate the state of the art and numerous problems, which require solution, are indicated.

INTRODUCTION

A launch vehicle is one of the most efficient structures that has been devised for transportation. In table 72–I are shown weights of various major components of a launch vehicle compared with those of other means of transportation. As can be seen, the relative weight

TABLE 72–I.—*Relative-Weight Breakdown for Various Forms of Transportation*

	Propellant	*Propulsion*	*Payload*	*Structure*
Launch Vehicle	88	4	6	2
Airplane (Jet)	43	7	10	40
Ship	15	10	25	50
Automobile	3	22	25	50
Train (75-Car)	1	3	77	19

of the structure of the launch vehicle is exceedingly small compared with other transport structures. This small relative weight of structure is required to contain the propellant, support the engine, and support and protect the payload in the presence of very severe environments. The margin of safety is, consequently, exceedingly small.

The environment which this structure must resist includes many static and dynamic factors as illustrated in figure 72–1.

Before engine ignition, but after the gantry has been removed, ground winds can induce rather severe loads—both a steady drag load and a dynamic response in a direction mainly normal to the wind direction.

At engine ignition and launcher release, longitudinal transients are induced which can be rather severe and are important, not only from the standpoint of basic structural strength, but also with regard to effects on smaller components. Also, the engine noise in the presence of the ground is of high intensity and, for the larger vehicles, new problems are being uncovered.

During flight through the transonic to the maximum-dynamic-pressure flight regime, the thrust and various steady-state and oscillating aerodynamic loads become important. These inputs include high steady-state acceleration, boundary-layer noise, winds and wind shear, and static high-pressure peaks around geometric discontinuities at transonic speeds upon which are superposed buffeting loads. In this same flight regime, consideration must be given to the vehicle control in the presence of high-velocity horizontal winds such as the jet stream as well as the stability and the coupling of the control sensor with the flexibility of the vehicle. Another stability problem involves flutter, either of the components such as fins or of a localized area involving thin panels.

Finally, stresses from internal pressure are also present during the launch period.

The principal load-carrying element of large launch vehicles is the thin-walled circular cylinder. A question of primary importance, therefore, is how to construct cylinder walls most efficiently for a given launch-vehicle design. Clearly, the best wall type will depend on the relative magnitudes of the loads shown in figure 72–1. Figure 72–2 illustrates this point for a hypothetical case where the only loads considered are two of the primary steady-state loads—internal pressure and bending moment.

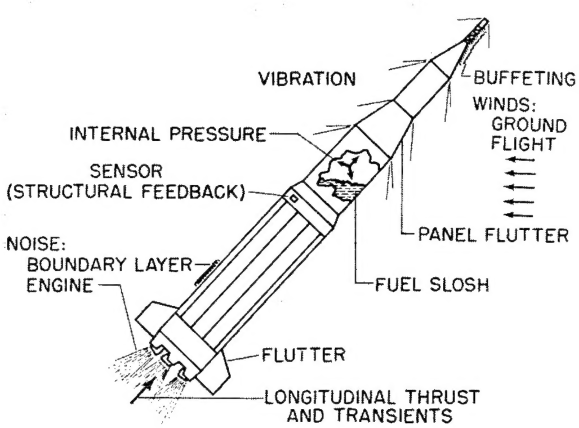

FIGURE 72–1.—Launch-vehicle problem areas.

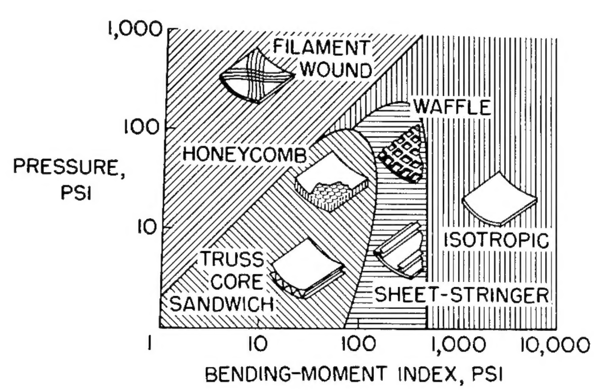

FIGURE 72–2.—Minimum-weight wall construction for bending of pressurized cylinders.

The plot in figure 72–2 shows the lightest form of construction which will carry pressure and bending loads without cylinder buckling or material yielding. The forms considered are filament wound, sandwich, stiffened skin, and simple isotropic walls. Note that, for high internal pressures as in solid-propellant launch vehicles, filament-wound construction is superior to the other types unless the applied bending-moment index is also large; then, the conventional, isotropic shell is lighter. For lower or zero internal pressures, as in liquid-propellant tanks or interstage structures, all types of wall construction have a range of efficient application, depending on the magnitude of the moment index.

Information of the type shown in figure 72–2 could obviously be very helpful in guiding the design of launch-vehicle structures. However, in deriving this figure, a very simple idealized structure has been assumed—a cylinder unobstructed by ends, cutouts, or other irregularities, and obeying simplified laws of behavior. Hence, the given boundaries must be modified or augmented for practical application. Further, other configurations and the many other static and dynamic loads must be taken into account. Thus, reliable and efficient design of launch-vehicle structures requires a wide knowledge of structural response to load plus an accurate knowledge of launch loads. This paper will touch briefly on some of these areas of necessary knowledge, their current state of development, and problems the solutions of which would contribute to their advancement.

SYMBOLS

EI_{sc}, EI_{cyl}	bending stiffeners for scalloped and cylindrical tanks, respectively
K	stress-concentration factor
L	length
R	tank radius
r	scallop radius
T	filament tension
T_{MAX}	maximum filament tension
t	thickness

SHELL BUCKLING

A prime requirement in launch-vehicle design is a shell-buckling criterion. Yet the designer's ability to predict buckling strengths of cylinders in axial compression or bending—loads of principal importance to launch vehicles—has been inadequate; there have continued to be large discrepancies between theory and experiment in spite of years of research effort. (See, for example, ref. 1.) Only very recently has there been uncovered what may be the chief cause of these discrepancies in the axial-compression case (ref. 2); this is illustrated in figure 72–3.

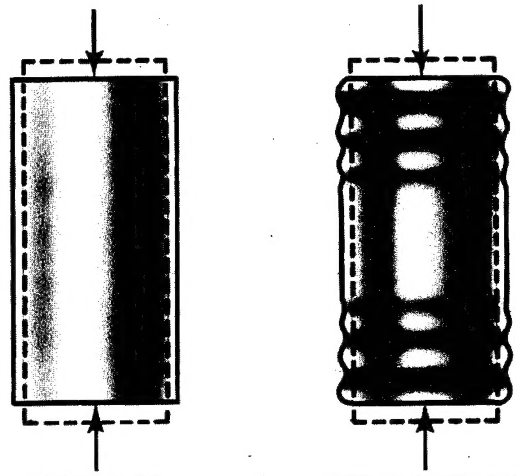

FIGURE 72–3.—Prebuckling state of axially compressed cylinders.

Consider for a moment, the illustration at the left in figure 72–3. In the classical linear theory and all other past theories, the cylinder is assumed to remain perfectly cylindrical with only uniform membrane stresses prior to buckling. Since an axially compressed cylinder tends to expand laterally, this assumption implies that, before buckling, the ends are free. But this condition is rarely found in practice; instead, the ends are restricted from lateral expansion by rings, bulkheads, or perhaps by the platens of a testing machine. This restraint induces prebuckling conditions that are widely different from those assumed in the classical theory; as illustrated at the right in figure 72–3 an axisymmetric, nonuniform deformation arises, accompanied by nonuniform stresses including bending stresses.

The importance of this nonuniform prebuckling state is illustrated by the example in figure

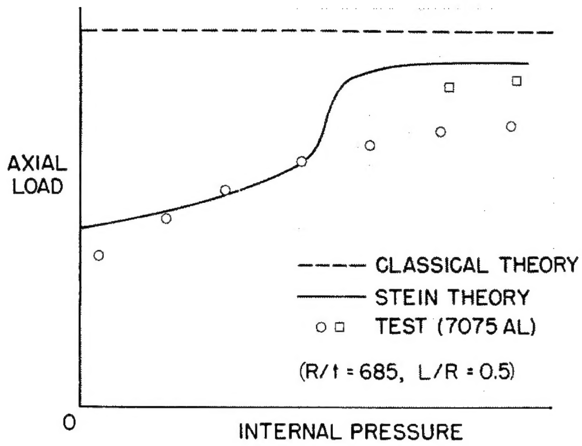

FIGURE 72-4.—Buckling of pressurized cylinders in axial compression.

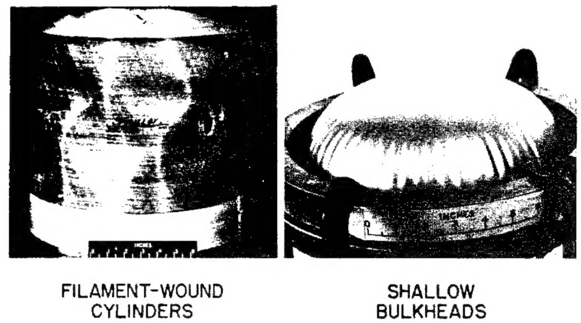

FIGURE 72-5.—New shell buckling problems of launch-vehicle structures.

72-4. In this figure are plotted combinations of axial load and internal pressure corresponding to buckling of a typical isotropic cylinder. The dashed line at the top is the prediction of classical theory whereas the solid curve is the prediction of a theory—termed here the "Stein theory" after its author—which takes account of the prebuckling state induced by simply supported ends. (See ref. 2.) The circles and squares represent test data from reference 3, which were obtained on two large cylinders of 7075 aluminum alloy.

Note that, at zero pressure, the Stein theory predicts buckling at approximately one-half of the load predicted by classical theory. This reduction is typical and corresponds roughly to the difference between classical theory and experiment. Although it differs in detail, the variation with pressure is also in general agreement with experiment.

The Stein approach to cylinder-buckling analysis begins with nonlinear cylinder equations and is, thus, quite complex. Nevertheless, additional calculations of this kind, extended to a wider range of parameters and to different boundary conditions, loading conditions, and configurations, would be well worthwhile.

While there is an evident need to improve the designer's ability to handle shell buckling problems of long standing, at the same time a variety of new problems important for launch-vehicle structures must be considered. Two examples are shown in figure 72-5.

Shown on the left in figure 72-5 is a filament-wound cylinder buckled by axial compression. This problem arises in upper stage motor cases before they are pressurized by ignition of their solid propellant. Surprisingly, almost no information on this problem seems to have been published. The cylinder shown is a test specimen from a current program of experiment and analysis. It consists of glass filaments in an epoxy matrix and is typical of construction in an upper stage motor case of the Scout launch vehicle. Preliminary results from this program are available (ref. 4), but much additional work is needed. For example, the calculation of wall stiffness properties from the properties of elastic fibers and an elastic-plastic matrix needs further study.

Another new and unique buckling problem involves the end bulkheads of fuel tanks. To minimize the length of interstage sections of launch vehicles, it is often desirable to utilize torispherical, Cassinian, or other shallow bulkhead shapes. In many practical cases, such bulkheads are put in a state of circumferential compression near their outer edges by internal pressurization. Thus, internal pressure can cause buckling of the bulkhead as shown by the photograph at the right in figure 72-5. As in axial compression of cylinders, the analysis of this buckling problem is complicated by the need for careful consideration of the prebuckling state. The torispherical bulkhead has been treated comprehensively in reference 5, but many shapes remain to be investigated.

STRESS ANALYSIS

The designer of launch vehicles cannot confine his attention to the primary steady loads and their gross effects. Many localized phenomena must also be taken into account. Examples are local variations in stress near openings, near tank end closures, and in the vicinity of concentrated forces. Most past theoretical research on such problems has been confined to linear analyses with lateral deflections of the shell wall assumed to be small compared with the shell thickness. Unfortunately, launch-vehicle shell structures are often very thin and the loads very large so that many of these problems need to be reconsidered on the basis of nonlinear, large-deflection shell theory.

Furthermore, there are problems of this type which have only been touched. Consider, for example, stresses in filament-wound structures. There is the problem of optimum design of motor-case end closures—the calculation of the proper shape and filament orientation to achieve uniform filament stress. (See, for example, ref. 6.) This problem has been explored for symmetrical shapes with central openings, but work is needed, for example, on optimum design of unsymmetrical end closures with multiple openings. There is also the problem of stress concentrations caused by broken filaments; this problem is illustrated in figure 72–6.

Figure 72–6 contains results of a basic study of a single flat layer of filaments embedded in a matrix. This filament sheet is assumed to have one or more broken fibers and to be loaded so that, far from the break, the tension on each filament is T. The maximum tension occurs adjacent to the break in the first unbroken fiber. Thus, the stress-concentration factor K is the ratio of T_{MAX} to T. This factor is plotted in figure 72–6 against the number of broken fibers up to a total of 6. The solid curve has been drawn through values obtained theoretically by assuming the sheet to be infinite, the materials elastic, and the matrix capable of transmitting only shear. (See ref. 7.)

To evaluate this theory, a brief series of tests has recently been run by George W. Zender and Jerry W. Deaton of the Langley Research Center on strips of dacron filaments in a foam rubber and Mylar matrix. Stress-concentration

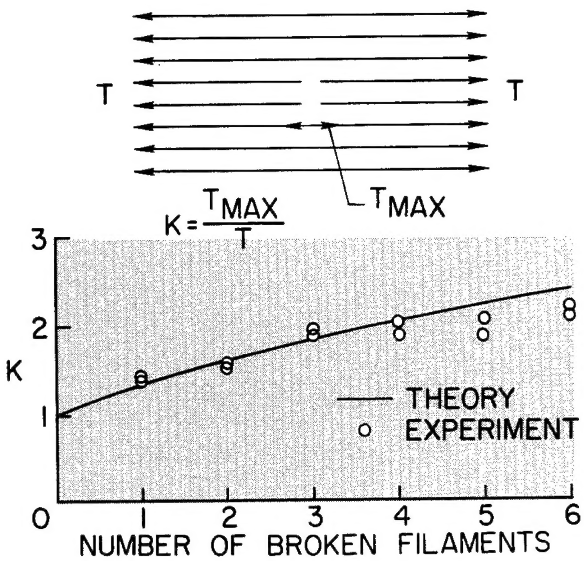

FIGURE 72–6.—Stress concentration in a filament sheet.

factors for the test strips were taken as the ratio of the fiber ultimate strengths with all fibers intact to the fiber strengths with one or more fibers broken. Two tests were run at each condition with the results shown by the circles in figure 72–6. The agreement with theory is good; one implication is that elastic stress concentrations must be seriously considered in design of filamentary structures with no careless reliance on plasticity to alleviate the effects.

This investigation represents a good beginning, but further studies are obviously needed if the consequences of broken fibers in a filament-wound motor case are to be fully understood. Such factors as multiple layers at different orientations and inelasticity of the matrix have not yet been studied. These complications pose a formidable challenge to the analyst.

PANEL FLUTTER

The local phenomena which influence launch-vehicle design may also include certain dynamic effects. For example, calculations indicate that panel flutter may be a matter of concern, but the issue is somewhat in doubt because experiments on cylinders and curved panels have so far failed to confirm theory. (See, for example, ref. 8.) On the other hand, a practical type of interstage structure, already in use in some of today's large launch vehicles, is the stiffened cylinder with thin skin designed to buckle early in flight. The

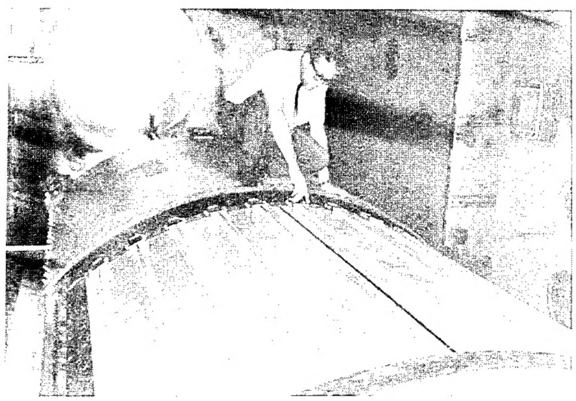

FIGURE 72-7.—Launch-vehicle interstage structure.

skin panels of such interstage structures might well be especially susceptible to flutter. This possibility is currently being explored by tests on the structure shown in figure 72-7.

The photograph shows a quarter segment of a full-scale launch-vehicle interstage structure installed in the Langley 9- by 6-foot thermal structures tunnel. The structure is a stiffened cylindrical shell with rings on the inside and stringers on the outside. While data from these tests are not yet available, flutter has been observed in preliminary runs with the panels in a buckled condition. Thus it appears that more work is warranted on panel flutter, especially of buckled flat and curved panels.

NOISE

It is appropriate at this point to direct attention to another local dynamic problem—the effect of noise. The two major sources of noise are the propulsion system, particularly at lift-off, and aerodynamic noise during flight due to boundary-layer buildup and flow around corners and blunt objects. (See ref. 9.) The spectra of aerodynamic noise peak at a relatively high frequency and are important with regard to local panels and small-equipment response. This topic is important to reentry vehicles as well as launch vehicles and is discussed in more detail in reference 10. The present paper will concentrate on new problems which are connected with the increasing size of launch vehicles.

Noise is important at the time of launch, particularly for the larger vehicles now in the

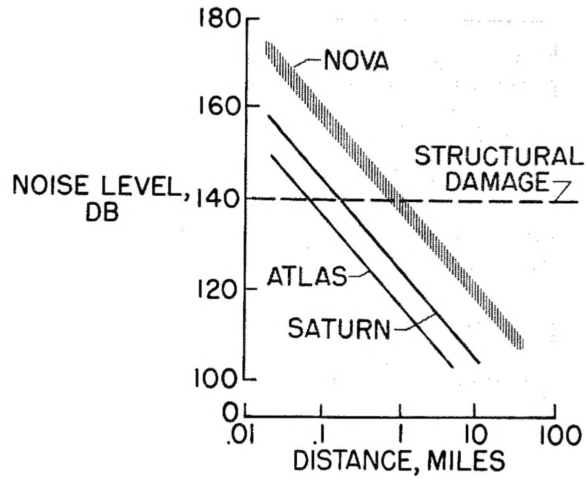

FIGURE 72-8.—Launch noise levels.

planning stages for manned space exploration. Because of the high thrust ratings, very intense noise fields will be generated and will extend to large distances from the launch complex. There are two major implications: the first is the impingement of this noise field on the vehicle itself and on launch vehicles installed in adjacent launch towers for later flight; and the second is the effect on the surrounding buildings and community. In figure 72-8, noise levels are plotted as a function of distance from the launch site for the Atlas, Saturn, and Nova classes of vehicles (ref. 11). Also shown is a horizontal line corresponding to noise levels at which damage has occurred. The position of this line is the subject of research and more work will have to be done to establish its location for various types of structures. It can be seen from figure 72-8 that damaging noise levels may extend outward as much as a mile from a Nova launch site; incidentally, it is this consideration that has determined to a large extent the amount of additional property purchased adjacent to launch sites in the Cape Canaveral area.

Another significant feature of the launch-vehicle noise problem is its frequency spectra; these are a function of the size of the vehicle as illustrated in figure 72-9. The noise generated has a continuous spectrum with a single broad peak as indicated in the sketch at the upper right. The frequency at which the spectrum peaks is plotted on the vertical scale against launch-vehicle thrust on the horizontal

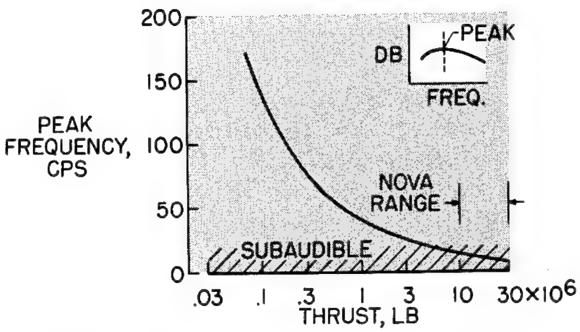

FIGURE 72–9.—Launch-vehicle noise spectra.

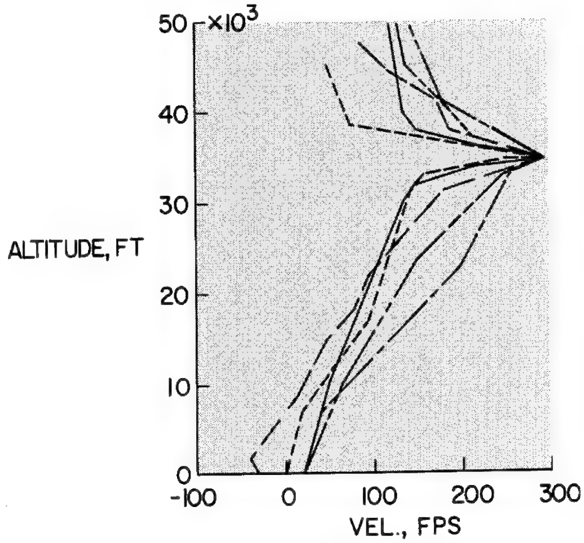

FIGURE 72–10.—Synthetic wind profiles.

scale. It can be seen that the vehicles having higher thrust have noise spectra which peak at low frequencies and, in fact, much of the noise may be in the subaudible frequency range as indicated by the cross-hatched area. These low frequencies—of the order of 10 cps—are in the range of the response frequencies of launch-vehicle structures as well as many building structures. For this reason, a large, low-frequency-noise test facility is being constructed at the Langley Research Center to extend the knowledge of this area.

WIND VELOCITY AND VEHICLE RESPONSE

The preceding sections of the present paper have been concerned with phenomena that affect launch-vehicle components. Attention will now be directed to some inputs and responses which involve the complete vehicle.

The horizontal wind through which the vertically rising vehicle must fly constitutes one of the largest sources of loads that the structure must resist. This is because maximum wind velocities and flight maximum dynamic pressure occur at very nearly the same altitude. Thus, the product of the dynamic pressure and the increased angle of attack resulting from these high winds induces very large bending moments on the vehicle.

For the most part, launch vehicles have been designed on the basis of the so-called "synthetic wind profile." This is a wind-velocity profile that has been generated from weather-balloon soundings and which represents the most severe wind and shear conditions to be expected in some given large percentage of cases, such as 99 percent.

An illustration of the multiplicity of some of these design profiles is shown in figure 72–10 where wind speed is plotted as the abscissa and the altitude is plotted as the ordinate. Note the large variations between these various design profiles. The control and load response of a vehicle is determined by "flying" the simulated vehicle on a computer through these design winds. Some designers also fly the simulated vehicle through a one-minus-cosine gust and add this loading to that determined by flying through the synthetic profile. Neglected in this process is the real finer grained wind-velocity structure to which the vehicle could dynamically respond.

In an attempt to fill the gap in knowledge of the fine-grain wind structure, a smoke-rocket technique has been developed. (See ref. 12.) This procedure is based on the near-vertical launching of a small rocket which has as its payload a smoke-producing agent. Photographs of the trail are taken every few seconds from 2 or 3 locations, usually about 10 miles from the launch site. The velocity may then be determined from the measurements of space variation of the trail with time. Two components of a typical profile, as determined from a trail, are shown in figure 72–11. Note in particular the fine-grain structure of the velocity distribution. Measurements are now being made at both the NASA Wallops Station

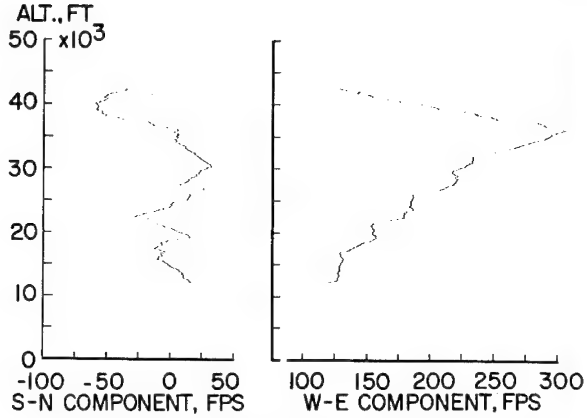

FIGURE 72-11.—Smoke-trail wind velocities.

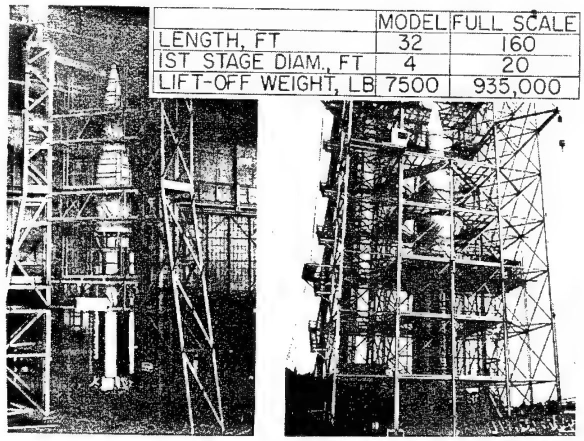

FIGURE 72-12.—Saturn vibration-test vehicles.

launching site and at the Atlantic Missile Range, where about 100 smoke-trail firings are planned. In addition, recent advances in the balloon technique will provide additional statistical information.

The question arises: How does the designer use this new data? One procedure would be to fly the vehicle on a computer through each of the measured winds, from which motion and load response would be obtained. Thus, the probability of exceeding a certain level of a response such as bending moment could be obtained. This procedure would require a large amount of computer time and other approaches should be sought. The most obvious technique would be the use of random-process theory.

Aircraft dynamic response is being successfully treated as essentially a stationary random process. Launch-vehicle flight, on the other hand, is definitely a nonstationary process since such factors as vehicle mass, atmospheric density, and Mach number are rapidly changing. Thus, while the detailed wind velocities now being measured by the smoke-trail method will provide the basic input data, the numerical labor will be very great in utilizing these data with the present limited knowledge of nonstationary random processes. Attempts should be made to review the present techniques with a view toward reducing the numerical labor and providing a practical design tool.

VIBRATIONS AND DYNAMIC MODELING

Before dynamic loads and responses can be predicted, or the control system designed, the lateral vibration modes and frequencies of a complete launch vehicle must be known. Some of the newer configurations are quite unconventional and exhibit unusual vibration characteristics which are extremely difficult to predict analytically. The difficulties of determining these vibration characteristics experimentally, on full-scale hardware in simulated flight, are obvious when vehicles the size of Saturn are considered. These considerations have led to the concept of replica modeling as a tool for launch-vehicle design.

The Langley Research Center has designed, constructed, and tested a 1/5-scale replica model of the Saturn SA-1 launch vehicle in an attempt to develop a technology for launch-vehicle dynamic models as well as to investigate the vibration characteristics of clustered configurations. (See ref. 13.) The 1/5-scale model is shown on the left in figure 72-12. A full-scale Saturn (SAD-1), suspended in a test tower to simulate free-free boundary conditions, is shown on the right. The model is 32 feet tall and weighs 7,500 pounds, compared to 160 feet and almost 1,000,000 pounds for the full-scale vehicle. The model was designed by using replica scaling techniques which required that joints, cutouts, fittings, and so forth—with stiffnesses that could not be accurately predicted—be duplicated by dimensional scaling.

An example of the vibration-test results and a comparison with full-scale results are shown in figure 72-13. Results shown are for the first free-free bending mode, at a weight condition

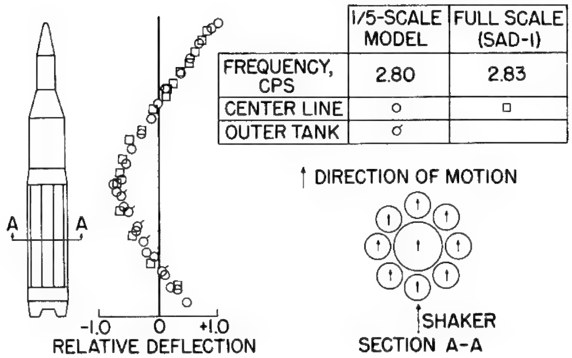

	1/5-SCALE MODEL	FULL SCALE (SAD-1)
FREQUENCY, CPS	2.80	2.83
CENTER LINE	o	□
OUTER TANK	ơ	

FIGURE 72-13.—First vibration mode at maximum dynamic pressure.

corresponding to the maximum-dynamic-pressure point in the launch trajectory. A scaled frequency of 2.80 cps was measured on the model, compared with 2.83 cps on the full-scale vehicle. The mode shapes measured on the model and on the full-scale vehicle agree very well as indicated by the circles and squares plotted in the figure. The flagged circles in the area of the first stage represent points measured along an outer tank in the cluster and indicate that these outer tanks follow the center-line motion. This tank motion is further illustrated by the cross-sectional sketch of the first stage, where the arrows indicate the motion of the various tanks within the cluster. All the tanks are seen to move together, with a resulting mode shape very similar to a beam bending mode.

A more complicated vibratory response is illustrated in figure 72-14. This is the mode shape at the second resonant frequency of the vehicle. The model frequency was 5.20 cps compared with 5.68 cps for the full-scale vehicle—less than a 10-percent variation. Again, circles represent model data, squares represent full-scale data, and flagged symbols indicate deflections measured on an outer tank. Note the different behavior of the outer and inner tanks within the cluster. This is shown better by the arrows on the first-stage cross section at the right. The center tank is seen to deflect in one direction while the outer tanks tend to move tangentially, but predominantly opposite to the motion of the center tank. This unconventional mode, which results from the clustered-tank construction of the first stage, has been termed a "cluster" mode. Notice that, when circles and squares are compared, model behavior is essentially the same as that of the full-scale vehicle.

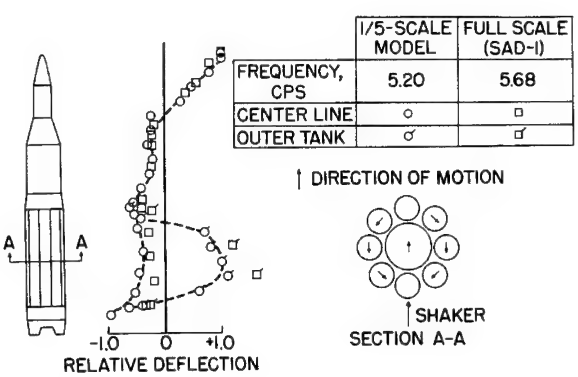

	1/5-SCALE MODEL	FULL SCALE (SAD-1)
FREQUENCY, CPS	5.20	5.68
CENTER LINE	o	□
OUTER TANK	ơ	□'

FIGURE 72-14.—Second vibration mode at maximum dynamic pressure.

The results in figures 72-13 and 72-14 indicate that dynamic models can be used to determine the vibration characteristics of complex launch vehicles. The unusual vibration characteristics of a particular clustered-booster arrangement are also illustrated. As new configurations evolve, it is anticipated that dynamic modeling techniques may be used to great advantage to study their dynamic structural properties.

CONCEPTS AND SYSTEM

This final topic will require an expanded viewpoint including more elements of the vehicle system—specifically, fuel slosh, control frequency, and their relationship to the lateral vibration modes. Attention will be focused on a promising new configuration—the scalloped tank—and the change in frequency spectrum from a cylindrical-tank vehicle to this new configuration will be indicated. A cross section of the scalloped tank is shown in figure 72-15; it consists essentially of a series of sectors of circles tied together by radial webs.

The primary and overriding reason for considering this configuration is the problem of fuel slosh. Since about 90 percent of the weight of a launch vehicle may be liquid, the stabilization of this large mass in cylindrical tanks by conventional means—for instance, by annular baffles connected to the outer walls of the cylindrical tank—imposes a rather severe weight penalty. Therefore, attempts should be

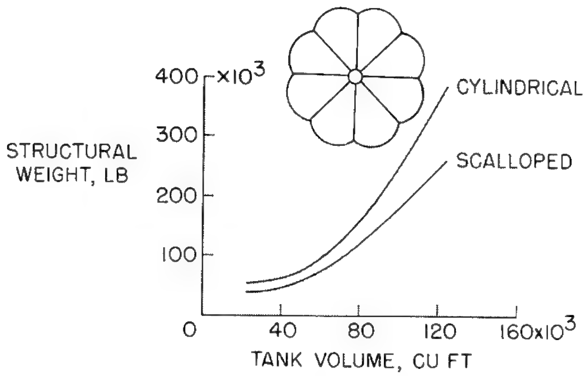

FIGURE 72–15.—Comparison of scalloped- and cylindrical-tank weights.

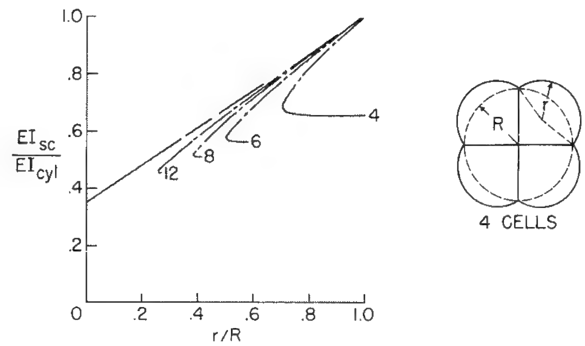

FIGURE 72–16.—Ratio of scalloped- to cylindrical-tank stiffness.

made to utilize this baffle material so that it will provide structural strength as well as reduce the fuel slosh effects. The scalloped-tank concept provides baffling by means of the radial webs which act also as structural tension members. On a two-dimensional basis (neglecting end effects and cylindrical-tank baffling), the weight of a cylindrical tank and a scalloped tank is the same if the same volume is enclosed and if the same internal pressure and material stress level is maintained in both tanks. A more realistic estimate of the weight of the two configurations (from ref. 14) is shown in figure 72–15 in which the tank ends have been accounted for as well as the required baffling in the cylindrical tanks. The cylindrical tank weighs about 25 percent more than the scalloped tank at smaller tank volumes and about 33 percent more for the largest volume considered.

Important aspects of the scalloped tank from the fuel-slosh viewpoint are the reduction of the effective fuel mass and, particularly, the elimination of any possibility of a swirling or rotary motion of the fluid which can be a dangerous and insidious fuel motion.

These advantages are, of course, not without certain penalties. First, fabrication of the tank becomes a much greater problem, that is, the complexity may increase the cost of manufacture. Also, the bending stiffness of the scalloped tank is decreased relative to that of the cylindrical tank as shown in figure 72–16 for several scalloped arrangements, including 4-, 6-, 8-, and 12-segmented tanks. The stiffness relative to that of a cylinder is plotted against the ratio of the scallop radius to the tank radius. As the number of segments increases, the stiffness is reduced. This reduction in stiffness results in a reduction in the frequency of the lateral modes and has an impact on both control-system design and the dynamic response due to gusts.

At the left of figure 72–17 is shown the variation in frequency of several important factors for a cylindrical tank plotted against flight time—for example, pitch (this compares with the more familiar airplane short-period frequency), fuel slosh, and first bending for a typical large launch vehicle. Baffling is required for stabilization in this case where the slosh and pitch frequency are very close.

Now, consider what happens to these frequencies for an 8-segmented scalloped tank. The results for this hypothetical configuration appear as shown on the right of figure 72–17. Note that the frequency curve for fuel slosh has been raised considerably (see ref. 15) and from a rigid-body control standpoint results in a more desirable situation, since the fuel-slosh

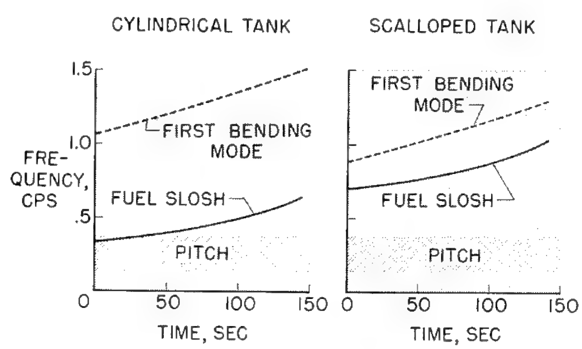

FIGURE 72–17.—Variation of frequency with flight time.

frequency is beginning to uncouple from the pitch frequency. At the same time the reduced stiffness has resulted in a reduced first bending frequency as indicated by the lowering of the frequency curve on the right side and thus introduces the possibility of a coupling between fuel slosh and the lateral vibration mode; this constitutes an area requiring research.

This exercise on the scalloped configuration has been made to indicate the type of thinking that must be pursued in investigating any particular configuration; that is, the complete system must be examined and the coupling of apparently unrelated elements must be sought out and evaluated.

CONCLUDING REMARKS

In this paper some of the branches of the technology needed in reliable and efficient design of launch-vehicle structures have been considered. Examples have been given to indicate the current state of the art and various problems for which solutions are needed have been mentioned; for the most part work more of an analytical than of an experimental nature has been indicated.

Among the problems considered were shell buckling and areas where analyses are needed of new shell configurations which have become important in launch-vehicle design. New and important problems of stress analysis—for example, stress concentrations in filamentary structures—have been pointed out, and the need for further studies of flutter of curved panels—especially in a buckled state—has been indicated. For the noise problem, work is needed involving the response of structures to the predominantly low-frequency noise of the largest launch vehicles and, for the determination of vehicle response to winds, a principal need is the development of a practical procedure for application of nonstationary random-process theory. Vibration analysis of clustered structures is needed, and finally, so is the conception and study of new configurations for application to the next generation of launch vehicles.

REFERENCES

1. Fung, Y. C., and Sechler, E. E.: Instability of Thin Elastic Shells. Structural Mechanics, J. Norman Goodier and Nicholas J. Hoff, eds., Pergamon Press (New York), 1960, pp. 115–168.
2. Stein, Manuel: The Effect on the Buckling of Perfect Cylinders of Prebuckling Deformations and Stresses Induced by Edge Support. Collected Papers on Instability of Shell Structures—1962. NASA TN D–1510, 1962, pp. 217–227.
3. Dow, Marvin B., and Peterson, James P.: Bending and Compression Tests of Pressurized Ring-Stiffened Cylinders. NASA TN D–360, 1960.
4. Card, Michael F., and Peterson, James P.: On the Instability of Orthotropic Cylinders. Collected Papers on Instability of Shell Structures—1962. NASA TN D–1510, 1962, pp. 297–308.
5. Mescall, John: Stability of Thin Torispherical Shells Under Uniform Internal Pressure. Collected Papers on Instability of Shell Structures—1962. NASA TN D–1510, 1962, pp. 671–692.
6. Zickel, John: Isotensoid Pressure Vessels. ARS Jour., vol. 32, no. 6, June 1962, pp. 950–951.
7. Hedgepeth, John M.: Stress Concentrations in Filamentary Structures. NASA TN D–882, 1961.
8. Stearman, R., and Fung, Y. C.: Experiments on the Stability of Circular Cylindrical Shells in a Supersonic Flow. GALCIT SM 62–36, 1962.
9. Hilton, David A., Mayes, William H., and Hubbard, Harvey H.: Noise Considerations for Manned Reentry Vehicles. NASA TN D–450, 1960.
10. Mathauser, Eldon E.: Research, Design Considerations, and Technological Problems of Structures for Winged Aerospace Vehicles. NASA-University Conference on the Science and Technology of Space Exploration, vol. 2, 1962, pp. 499–510.
11. Regier, Arthur A., Mayes, William H., and Edge, Phillip M., Jr.: Some Noise Problems Associated With the Launching of Large Space Vehicles. Presented at Annual Meeting of Armed Forces-National Research Council Committee on Hearing

and Bio-Acoustics (Washington, D.C.), Nov. 3, 1961. (To be published in Sound, Nov.-Dec. 1962.)

12. HENRY, ROBERT M., BRANDON, GEORGE W., TOLEFSON, HAROLD B., and LANFORD, WADE E.: The Smoke-Trail Method for Obtaining Detailed Measurements of the Vertical Wind Profile for Application to Missile-Dynamic-Response Problems. NASA TN D-976, 1961.
13. MIXSON, J. S., and CATHERINE, J. J.: Investigation of Vibration Characteristics of a *1/5*-Scale Model of Saturn SA-1. Shock, Vibration and Associated Environments—Pt. IV. Bull. No. 30, Office of Sec. of Defense, Apr. 1962, pp. 30–39.
14. STERETT, JAMES B., JR.: Shell Stability Problems in the Design of Large Space Vehicle Boosters. Collected Papers on Instability of Shell Structures—1962. NASA TN D-1510, 1962, pp. 57–66.
15. ABRAMSON, H. NORMAN, GARZA, LUIS R., and KANA, DANIEL D.: Liquid Sloshing in Compartmented Cylindrical Tanks. ARS Jour., vol. 32, no. 6, June 1962, pp. 978–980.

Research, Design Considerations, and Technological Problems of Structures for Winged Aerospace Vehicles

By Eldon E. Mathauser

ELDON E. MATHAUSER, *Head of the Structural Materials Branch, Structures Research Division, NASA Langley Research Center, received his Bachelor of Science degree in civil engineering in 1944 and his Master of Science degree in engineering mechanics in 1950, both from the University of Nebraska.*

Mathauser was an instructor in the Department of Engineering Mechanics at the University of Nebraska from 1946 to 1951. Since joining Langley in July 1951, he has specialized in research on structures and materials for high temperature applications. He is author of approximately 20 NASA technical papers on structures and materials with emphasis on behavior and performance at high temperatures. He is a member of the Institute of the Aerospace Sciences, Sigma XI honorary scientific society, and Sigma Tau honorary engineering society, and is a registered professional engineer in the state of Nebraska.

SUMMARY

Research, design considerations, and technological problems of structures for winged aerospace vehicles are discussed and areas in need of further research are explored. The presentation includes structural approaches required to cope with the high nonuniform temperatures and the influence of such factors as flutter, acoustic fatigue, and materials selection on the structural design.

INTRODUCTION

Considerable interest is being displayed at the present time in winged aerospace vehicles. These vehicles possess various desirable operating characteristics such as high lift-drag ratio, maneuverability, and horizontal landing capability. In this paper structural concepts appropriate for winged aerospace vehicles will be discussed. The presentation will include structural approaches required to cope with the high nonuniform temperatures and the influence of several factors, such as flutter, fatigue, and materials selection, on structural design will be indicated.

DESIGN BASIS

Winged Aerospace Vehicle Configurations

Three types of winged aerospace vehicles that will be considered are shown in figure 73–1. A research airplane characterized by the X–15 (ref. 1) is shown at the upper left, a reentry glider representative of the X–20 Dyna-Soar (ref. 2) is shown in the upper right, and a large hypersonic airplane (ref. 3) that may be capable of sustained flight at hypersonic speeds or may have orbital capability is shown in the lower view. The structural approaches for these vehicles have many common features. All experience moderate to severe aerodynamic heating and utilize radiation-cooled structural designs. All structures are essentially metallic and are intended for reuse with minimum refurbishment.

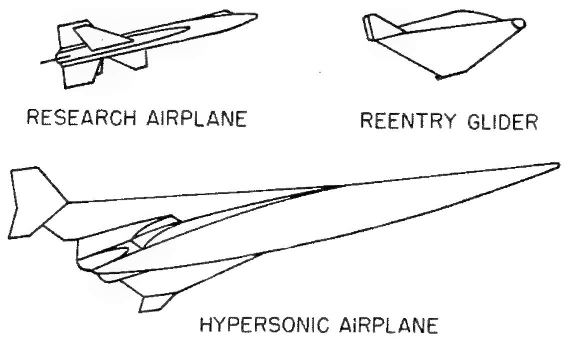

FIGURE 73-1.—Winged aerospace vehicles.

The operational characteristics of these vehicles are significantly different. The research airplane is carried aloft by another airplane and launched at altitude. The reentry glider may be launched with a ground-based booster. The hypersonic airplane carries its own fuel and possesses conventional horizontal take-off capabilities.

Flight Corridors for Winged Aerospace Vehicles

Before a discussion of structural problems is undertaken, a brief look will be taken at the flight corridors for these vehicles. Figure 73–2 indicates the flight corridors in terms of altitude and velocity. The shaded area indicates the region that can be explored by the X–15 research airplane. (See ref. 4.) The glider is launched along an exit trajectory as shown and returns within the indicated reentry corridor. The lower limits of the reentry corridor are defined partly by temperature and dynamic pressure. The 4000° F temperature line defines a radiation equilibrium temperature for a 1-foot-diameter nose with an emissivity of 0.8. Note that the reentry glider does not experience severe heating during exit because the exit corridor does not appear close to the indicated temperature line. It is significant to note that the exit corridor is near the curve for 2,000 pounds per square foot dynamic pressure. This fact suggests the possibility that flutter may be a problem during exit. The highest structural temperatures occur at the point of tangency between the flight corridor and the temperature curve.

No specific flight corridor is indicated for the hypersonic airplane. It is expected that the hypersonic airplane will operate along a dynamic pressure curve and along a temperature line. If the vehicle possesses orbital capability, reentry with a hypersonic airplane would be made in approximately the same corridor as that for the glider.

Structural Temperatures

The most pressing structural problems arising from operations in the indicated flight corridors come about because of the serious aerodynamic heating. The magnitudes of the temperatures that can result are shown in figure 73–3. A reentry glider is shown with surface-radiation equilibrium temperatures indicated for several areas of the vehicle. The nose temperature may approach 4000° F, the leading edges 3000° F, the underside 2500° F, and the leeward side 1000° F to 1500° F. The high structural temperatures that may be achieved by aerospace vehicles produce signifi-

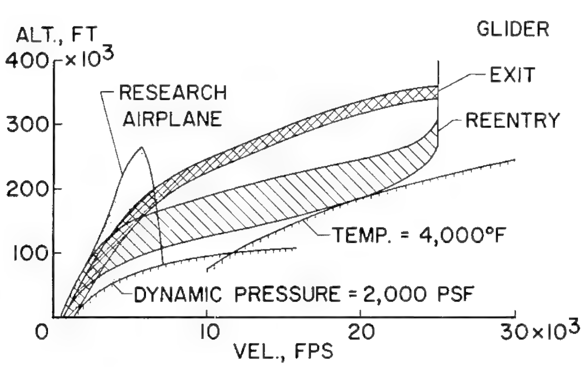

FIGURE 73–2.—Flight corridors for winged aerospace vehicles.

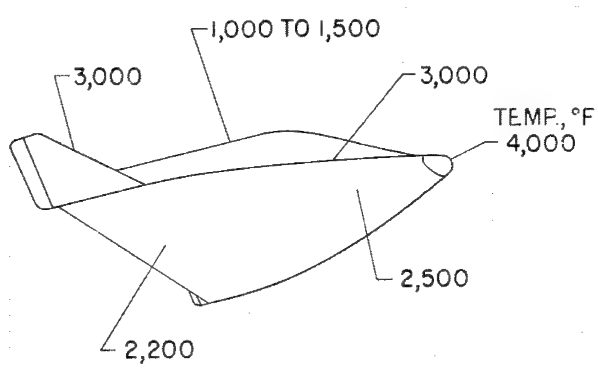

FIGURE 73–3.—Surface radiation equilibrium temperatures for a reentry glider.

cant design problems. Of equal significance is the fact that highly nonuniform temperatures occur that produce severe structural deformations and introduce thermal stresses. Temperature differences of over 1000° F are indicated between the lower and upper areas of the body. Because of such large temperature differences, new design approaches and special construction concepts are required. This paper is primarily devoted to design concepts required for structures subjected to severe nonuniform temperatures.

DESIGN CONCEPTS

Design Concepts for Primary Structure

As may be expected, no single structural concept is applicable for the various types of winged aerospace vehicles of concern here. Figure 73–4 indicates two general approaches on which the structural design may be based. (See ref. 5.) Shown at the left is the hot-structure concept in which the structure operates near the equilibrium temperature and supports applied loads adequately. The other concept labeled "protected structure" consists of a thermal protection system that maintains low structural temperatures so that the imposed loads are carried by a relatively cold primary structure. The hot structure avoids the difficult design problems associated with the thermal protection system on the protected structure; however, other significant difficulties including materials and thermoelastic problems are introduced. The primary load-carrying structure associated with the protected-structure concept can be designed largely on the basis of existing technology associated with structures for current aircraft. For this reason no further attention to the cold primary structure design is given. Further considerations of thermal-protection systems with emphasis on heat-shield design will be presented subsequently.

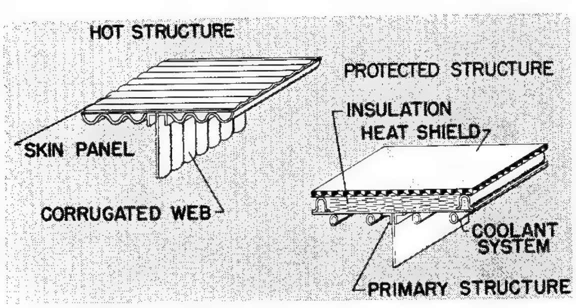

FIGURE 73–4.—Structural concepts for winged aerospace vehicles.

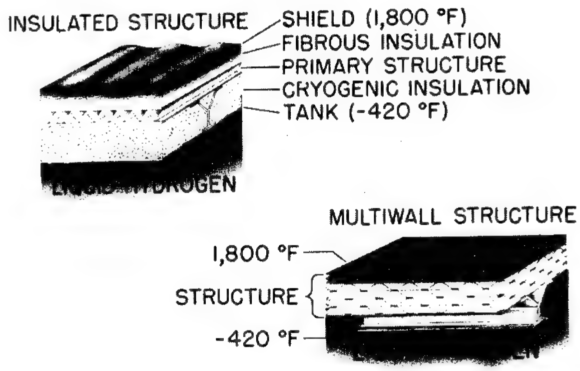

FIGURE 73–5.—Structural concepts for hypersonic airplane. Cryogenic fuel tank area.

The advantages and limitations of these two approaches have been the subject of numerous studies. (See ref. 6.) No clear choice exists between the two design concepts. The resulting designs are generally competitive weightwise and both concepts appear to be feasible.

Structural Concepts for Cryogenic Fueled Vehicles

Because vehicles that utilize cryogenic fuels pose unusual structural requirements, special considerations will be given here to possible design concepts. Two such concepts are indicated in figure 73–5. An insulated type of structural concept indicated in the left-hand view consists of a heat shield that may be a superalloy for temperatures up to 1800° F and refractory metal for higher temperatures, fibrous high-temperature insulation, primary structure, cryogenic insulation, and, lastly, the tank containing cryogenic fuel which is assumed in this case to be liquid hydrogen. The temperature of the primary structure is dependent in part on the relative thicknesses of the cryogenic and fibrous insulation utilized. A low primary-structure temperature appears desirable to take advantage of favorable material properties and to minimize thermal-expansion problems. This type of construction requires essentially three leak-tight shells including the internal hydrogen tank, the primary structure to preclude

liquification of air that enters the cryogenic insulation area, and lastly, the heat shield to prevent trapping and freezing of moisture within the fibrous insulation area.

In the right-hand view a multiwall design approach is indicated. This design is unique because the thermal-protection and load-carrying functions are combined into one integral component. The design consists of alternate layers of flat and dimpled sheets joined together by welding. The insulating effect is produced by the multiple-layer reflective sheets. This structural concept possesses several advantages over other approaches including effective utilization of different sheet materials to give optimum strength-weight ratios, possible improvement in structural reliability through integration of the thermal-protection and load-carrying functions, improved resistance to dynamic pressures, and good protection against meteoroid penetration.

The full potential of the multiwall concept has not been established. It is anticipated that thermal stresses associated with the large temperature differences through the wall thickness may be a major problem. Development of appropriate methods of analysis are required, as well as experimental investigations to verify the analytical methods.

Leading-Edge Approaches

Various types of designs that are representative of thermal-protection systems for leading edges of winged aerospace vehicles are indicated in figure 73–6. The nonmelting heat sink where some of the stagnation-region heat load is transferred rearward and then radiated represents one of the important leading-edge concepts. Its characteristics are readily amenable to analysis (ref. 5) and this approach has received extensive theoretical study. The leading edge of the X–15 research airplane is based on this approach. In the radiation approach, both metallic and ceramic designs are indicated. Recent advances in both coated refractory metals and in oxide ceramics indicate that the radiation approach to leading edges is feasible. The leading edge of the X–20 Dyna-Soar is based on the metallic radiation approach.

The internal cooling approach and the tran-

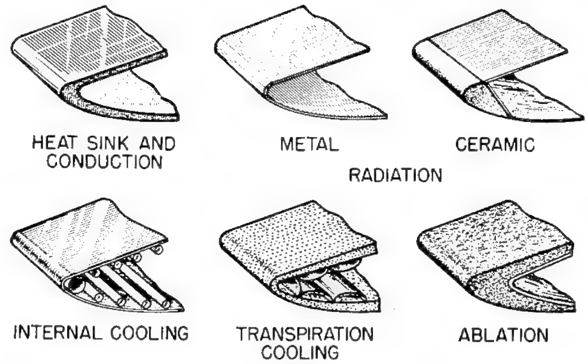

FIGURE 73–6.—Leading-edge approaches for winged aerospace vehicles.

spiration and film cooling approach may be expected to find application in some flight vehicles in which the shape of the edge must be accurately maintained during flight to achieve desired vehicle performance. Both of these concepts appear very promising; however, neither concept is in an advanced stage of development. Further efforts will be required to permit their utilization in flight vehicles. The ablation approach is of considerable interest and may also be utilized. The change in shape that accompanies the ablation process however may lead to undesirable vehicle performance in some cases. All of these leading-edge approaches appear to be feasible and are of current interest. No attempt will be made to compare these various concepts on a weight basis. In many cases, factors such as reusability, simplicity, and reliability will have important bearing on the type of approach utilized.

Application of Construction Concepts for Nonuniformly Heated Structures

Numerous construction concepts have been proposed to cope with severe nonuniform temperatures. These include corrugations, beads, and expansion joints. All of these approaches have been incorporated in a large structural model representative of a forward portion of a reentry glider. The model was fabricated at the Langley Research Center and was subjected to an extensive experimental investigation. (See ref. 7.) Figures 73–7 and 73–8 show the interior and exterior details of the model.

Figure 73–7 shows the internal structure of a model 12 feet long. The structure consists

of an approximately orthogonal arrangement of longitudinal beams and transverse frames. The loads from the exterior skin panels are transmitted to the transverse frames and the frames in turn transmit the loads to the two longitudinal beams. Corrugated shear webs are used in both transverse frames and longitudinal beams to resist shear loads and to permit differential thermal expansion between the top and bottom spar caps. Two different types of corrugations are utilized as shown. A conventional 60° corrugation was selected for the longitudinal beams and a special corrugation that permitted large flexibility at right angles to the transverse frames was selected for the transverse frames.

An external view of the model showing the skin panels attached is presented in figure 73–8. The skin panels are attached to the outside flanges of the transverse frames. Expansion joints can be seen extending around the model at approximately 2-foot intervals. These expansion joints as indicated consist of an omega-shaped metal strip that permits differential expansion between adjacent panels and also provides a tie between the panels so that their shear stiffness can be utilized to provide torsional stiffness for the model.

The skin panels as shown consist of two thin sheets seam-welded together. The external sheet is beaded lightly to stiffen it against local buckling and to preset a pattern for uniform deformation when thermal expansion is restrained across the corrugations. The inner sheet consists of ½-inch flat 60° corrugations.

This model has been subjected to numerous

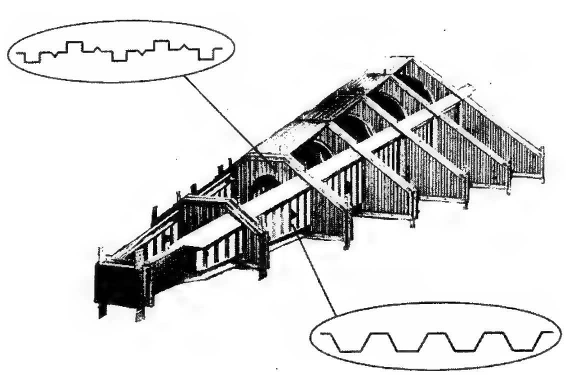

FIGURE 73–7.—Interior view of structural model.

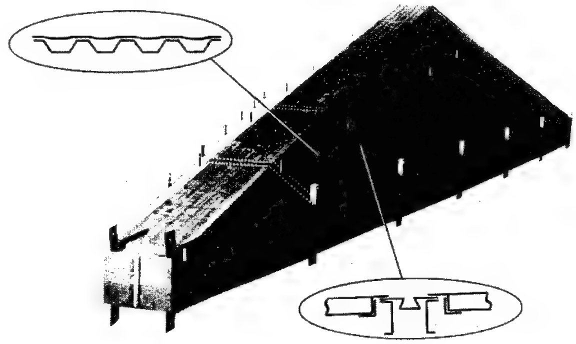

FIGURE 73–8.—Exterior view of structural model.

loading and heating tests with test temperatures ranging up to 1600° F. No significant structural damage was observed. It thus appears that the various structural concepts utilized in the model are practical for coping with both loads and high nonuniform temperatures.

Insulating Heat-Shield Concept

If the anticipated temperatures for the skin panels exceed the desired use temperatures, a possible method for coping with the high external temperatures is to provide a nonload-carrying insulating heat shield over the structural panels. With the proper amount of insulation, the load-carrying structure can be maintained within the useful temperature range for the material. Many different heat-shield concepts have been proposed. In this paper one typical design concept is described. (See ref. 8.) This typical design is indicated in figure 73–9. The shield consists of a lightly corrugated outer skin and then a layer of insulation. The primary structure is shown below the insulation. In the outer skin, nonuniform expansion is permitted to occur across the corruga-

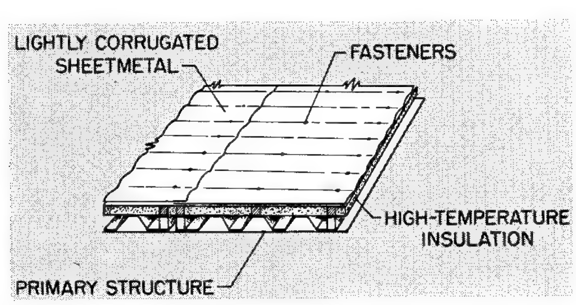

FIGURE 73–9.—Heat-shield concept.

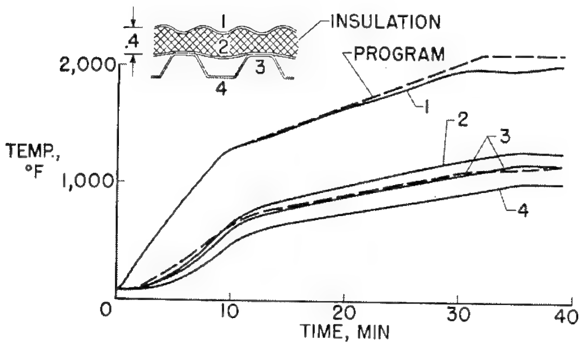

FIGURE 73–10.—Temperature-time history for heat shield.

tions by an increase or decrease in the amplitude or depth of the corrugations. In the other direction, expansion is permitted through the use of flexible supports at the ends of the corrugated outer sheet. The problem that must be coped with satisfactorily is to support the outer skin adequately so that it will survive in the airstream and will accommodate the thermal expansion resulting from the large temperature differences between the shield and structure. The aerothermoelastic environment imposed on the heat shield is usually very severe, and stiffness requirements to prevent panel flutter may generally dictate the design. (See ref. 4.) Adequate and properly spaced fasteners between the shield and primary structure must be provided.

The performance of a typical heat shield is shown in figure 73–10. The temperature-time history for the shield is shown. The upper dashed line (labeled "program") indicates a calculated temperature-time history for a point on the heat shield of a reentry glider. The experimentally applied temperature was obtained by program-controlled quartz-lamp radiators that heated the 2-foot-square panel. The response of the underlying structure is indicated by the solid curves and the predicted response by the dashed curve. Methods for predicting structural temperatures under conditions such as these are well established and have received extensive theoretical study. The adequacy of the theoretical methods is evidenced by the satisfactory correlation between theory and experiment.

This shield consisting of the outer corrugated sheet and attachment clips weighed approximately 1 pound per square foot. The insulation was quartz fiber 0.4 inch thick. Note that a temperature difference of approximately 1000° F existed between the shield and the internal structure during the period of maximum shield temperature. It is of interest to note that similar shields have been subjected to supersonic airflow with dynamic pressures up to 3,000 pounds per square foot and to noise environment ranging up to approximately 160 decibels. The shields have withstood these environments successfully.

OTHER FACTORS THAT INFLUENCE STRUCTURAL DESIGN

The discussion thus far has focused on structural designs for coping with the nonuniformly and highly heated vehicles. Several other factors that have a pronounced effect on the structural design will now be considered. These include flutter, fatigue, and materials selection.

Flutter

Because it has an important bearing on structural integrity, flutter is presently recognized as a critical problem area for winged aerospace vehicles. In this paper attention will be devoted to only one aspect of the general problem of flutter, namely, panel flutter. Panel flutter is of particular significance for structural surfaces of winged aerospace vehicles that are fabricated from thin sheets of high-strength high-density materials and are designed to carry small structural loads. It is recognized as a supersonic phenomenon, and several present-day aircraft have recently encountered panel flutter in flight at supersonic speeds. Let us consider the X–15 research airplane for a specific example. (See fig. 73–11.) The shaded areas, including the fairing panels along the sides of the fuselage and the vertical tail, have been affected and modified by considerations of flutter. (See ref. 4.) It was found that many of these panels required reinforcements as high dynamic pressures were explored in flight. Panels with corrugations normal to the airflow were particularly prone to flutter. In view of the importance of corrugations for exterior surface panels of aerospace vehicles, the first consideration is the influence of corrugation orientation relative to airflow on panel flutter.

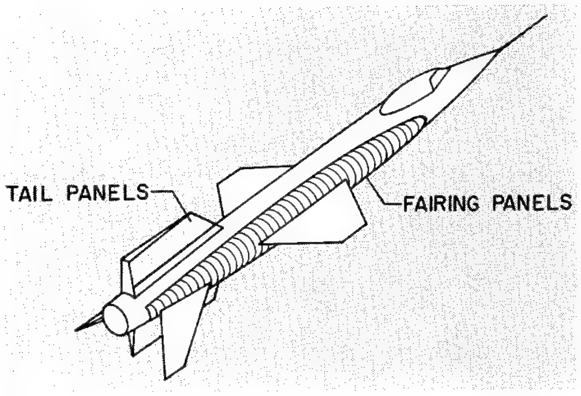

FIGURE 73-11.—Flutter areas on X-15 research airplane.

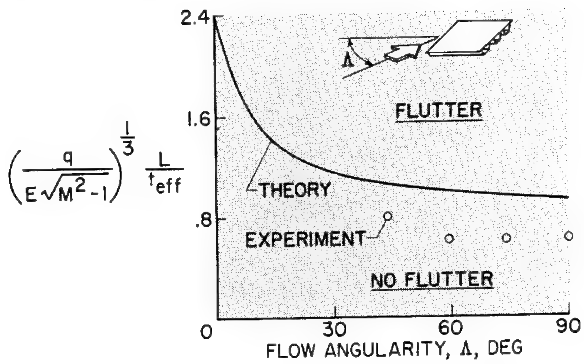

FIGURE 73-12.—Effect of flow angularity on flutter of orthotropic panels.

In figure 73-12 the panel-flutter parameter is plotted against the flow angularity. In this figure,

L	panel length
t_{eff}	effective panel thickness
q	dynamic pressure
M	Mach number
E	Young's modulus for panel material
Λ	flow angle measured in plane of panel relative to corrugation axes

The predicted flutter boundary is indicated by the curve and several experimental results are shown by the symbols. When compared with theory, the experimental data are low. The predicted flutter boundary was obtained from a four-mode solution of the orthotropic plate equation by assuming two modes in each of the orthogonal directions. (See ref. 9.)

Figure 73-12 demonstrates the strong influence of flow direction on orthotropic panel flutter. A particularly large decrease in resistance to flutter is indicated by the theory for small changes in flow direction from the corrugation axis. For example, for a 15° deviation in the flow direction the dynamic pressure estimated to produce panel flutter is approximately one-eighth of the magnitude indicated for zero flow angularity. This sensitivity to small variations in flow angularity would be of concern for vehicles that operate through large attitude changes with accompanying large variations in flow direction over the structural panels.

Attention will now be directed at two additional parameters that have significant influence on panel flutter. These parameters are panel midplane stress and pressure difference across the panel. The influence of these parameters will be discussed with the aid of figure 73-13. The ordinate is essentially the same panel-flutter parameter shown in figure 73-12, and the abscissa is a differential temperature ratio. The temperature increase in the panel due to aerodynamic heating is denoted by ΔT and a reference temperature that is proportional to the buckling temperature for the panel is denoted by ΔT_R. The parameter on the abscissa gives an indication of the magnitude of the midplane stress in the panel. The symbols represent flutter points obtained from a series of similar isotropic panels tested in a supersonic wind tunnel. The open symbols establish the flutter boundary for the panels in a flat and unbuckled condition, and the solid symbols define the flutter behavior when the panels were buckled. Note that it is possible for a panel to

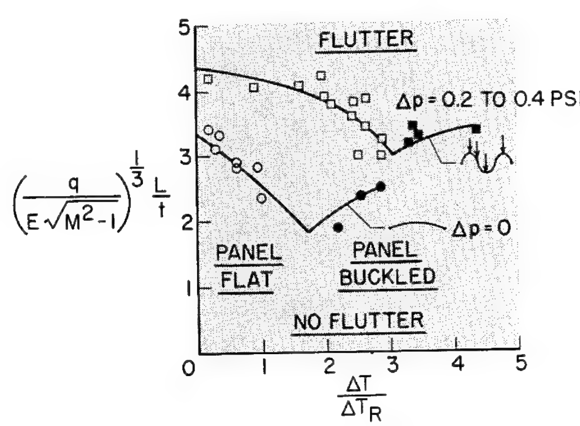

FIGURE 73-13.—Effects of midplane stress and differential pressure on panel flutter.

remain flat and flutter free until some midplane stress is developed during the aerodynamic heating. The panel then flutters, and eventually flutter may stop when the panel is in a buckled condition. The data shown by the lower curve correspond to a pressure difference across the panel Δp equal to zero. The upper curve indicates test data for similar panels that experience a pressure differential of 0.2 to 0.4 pound per square inch acting inward on the panels. This magnitude of pressure difference was sufficient to change the flutter boundary from the lower to the upper curve. In addition, the flutter mode changed from a standing-wave type for the lower boundary to a traveling-wave type for the upper boundary. Thus, a small pressure differential of approximately 0.2- to 0.4-pound per square inch was sufficient to produce a considerable change in the flutter mode and a change in the flutter boundary.

Figures 73–12 and 73–13 have identified three factors that have significant effect on panel flutter. Theoretical predictions of panel flutter to date do not generally show close correlation with experimental results; however, valuable analytical contributions are being made at the present time. It is hoped that present studies will be continued to improve our understanding of the panel-flutter problem.

Fatigue Aspects of Winged Aerospace Vehicles

Fatigue is recognized as a potentially important factor in the design of all modern lightweight flight vehicles. The specific role of fatigue in the design approach for winged aerospace vehicles is not clear although it appears that certain aspects such as acoustic fatigue will be of major concern. Acoustic fatigue problems may arise from either powerplant or aerodynamic boundary-layer noise. Attention will be devoted to the latter. Very little information is available at the present time to characterize the boundary-layer noise associated with hypersonic flight. On the basis of a large number of experiments, it appears that boundary-layer-noise pressures on a vehicle are generally proportional to the local dynamic pressures. (See ref. 10.) Figure 73–14 indicates the surface pressure level of the boundary-layer noise in

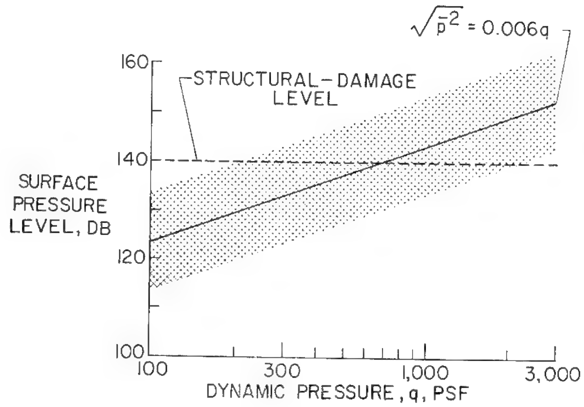

FIGURE 73–14.—Boundary-layer noise pressure levels.

decibels plotted against dynamic pressures that are of interest for winged aerospace vehicles. The solid line is given by the indicated equation in which the term $\sqrt{\bar{p}^2}$ is the mean-square value of fluctuating pressure and q is the dynamic pressure. A structural-damage level line is indicated at 140 decibels by the dashed line. The location of this line on the ordinate depends on the type of structural design, the duration of the noise pressure, and other factors.

The solid curve is derived mainly from experimental data at subsonic speeds. Recent wind-tunnel and flight tests at supersonic speeds have indicated that the surface pressure level may be either higher or lower as indicated by the cross-hatched band. (See ref. 11.) Insufficient experimental data exist, particularly at hypersonic speeds, to aid in establishing the proper relationship between these parameters; however, it is clear that boundary-layer noise increases with increasing dynamic pressure. It also appears that acoustic fatigue will become an increasingly severe problem for winged aerospace vehicles because of the use of high-strength thin-gage materials coupled with construction that will utilize large numbers of tiny weld joints that are potential sources for fatigue cracks.

The second aspect of the boundary-layer-noise problem is associated with determination of the structural response and estimation of fatigue life or damage. Studies in this area are based largely on experimental data. An example of structural fatigue damage that is determined experimentally (ref. 12) is given in figure 73–

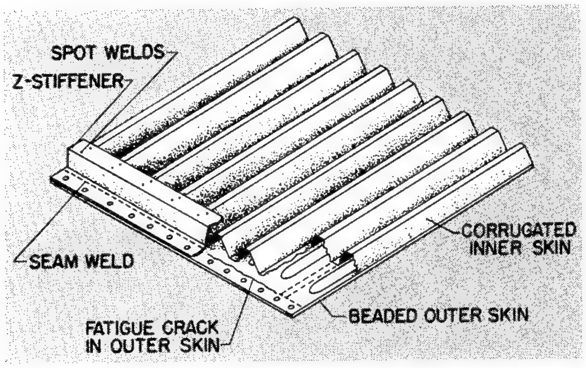

FIGURE 73-15.—Acoustic fatigue failure of corrugation-stiffened panel.

15. This figure shows a corrugation-stiffened panel utilized in an acoustic fatigue study to establish weaknesses in the panel design. This particular panel consisted of a lightly beaded outer skin, a corrugated inner skin seam-welded to the outer skin, and **Z**-stiffeners seam-welded to the outer skin and spot-welded to the corrugations. Acoustic fatigue tests were conducted at high noise levels for the purpose of determining the locations and types of failures. The tests determined that initial failure occurred in the spotwelds attaching the inner skin to the **Z**-stiffeners. Skin cracks were also observed near the end of the panel in the vicinity of the seam welds attaching the outer skin to the **Z**-stiffener. The results indicated were obtained at room temperature.

Figure 73-16 shows the results of a systematic series of acoustic fatigue tests that were made on corrugated-core sandwich panels fabricated from stainless steel. Sound pressure level is plotted against time to failure. Test temperatures of 450° F and 750° F are indicated on the dashed curves. The panels were approximately 15 inches square and were subjected to simultaneous heating and noise environment. The width of the small horizontal bars indicates the uncertainty in the actual failure time of the panels. The test temperatures noted adjacent to the bars at the top of the figure indicate lifetime results obtained at different temperatures at 162 decibels. These results show that the life of the sandwich panels, as expected, was influenced by the magnitude of the sound pressure level as well as by the temperature. The ability to predict life of complex structural components does not exist at the present time and considerably more effort will be required to bring about a better understanding of this problem.

Materials Influence on Structural Design

Attention will now be directed to materials to indicate their influence on vehicle design. It is recognized that progress in materials has substantial influence on design and performance of flight vehicles. Materials limitations are instrumental in establishing temperature limits as well as strength and stiffness capabilities. Some of the materials problems that have direct bearing on structural vehicle performance will be reviewed.

In figure 73-17 the variations of materials strength with temperature are indicated for several classes of structural materials of interest for winged aerospace vehicles. The data shown on the left apply to tensile strengths obtained from smooth specimens and the data on the right were obtained from specimens

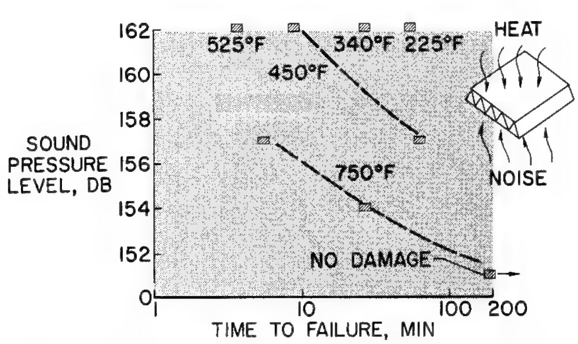

FIGURE 73-16.—Effect of noise level and temperature on time to failure of truss-core sandwich panel.

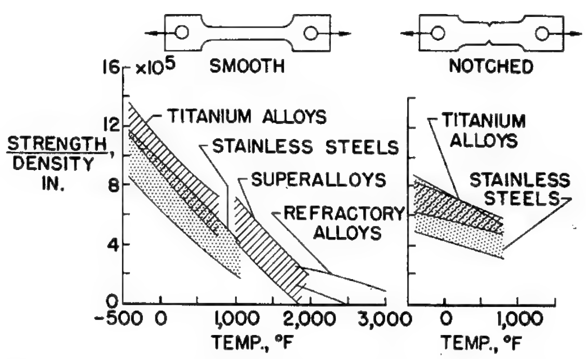

FIGURE 73-17.—Strength of structural materials determined from smooth or notched tensile specimens.

with external notches. (See, for example, refs. 13 to 15.) The strength-density ratio is plotted against temperatures ranging from liquid hydrogen temperatures to 3000° F. Titanium alloys, stainless steels, superalloys, and refractory metal alloys are shown. The shaded areas corresponding to each class of materials indicate the spread in tensile strength for various alloys within each class of materials. It appears that the most efficient structural design is obtained at liquid hydrogen temperatures, provided that it is possible to realize such high strength-density values. The indicated strength-density values will not be realized, however, because of the notch sensitivity of the material.

The shaded areas on the right indicate the sharp notch strength which is a measure of the sensitivity of the material to high stress concentrations or cracks. Data are shown only for titanium alloys and stainless steels. Note that at liquid hydrogen temperatures the sharp notch strength is approximately one-half of the smooth specimen strength. Information of this type on the superalloys and refractory metal alloys above 1000° F is practically nonexistent at present. The large decrease in strength attributed to sharp notches emphasizes the fact that high strengths of many materials cannot always be realized. It should be noted that strength data obtained from notched specimens appear useful for comparison purposes among various materials; however, the methods for utilization of this information in vehicle design are not established at the present time. Further study of this problem appears to be warranted.

A generally large materials effort is underway at the present time to determine the potential of refractory metals for aerospace vehicle applications. Among the many problems that must be overcome, oxidation of the refractory metals at their desired use temperatures above 2000° F is perhaps one of the most serious. Figure 73–18 indicates the progress that has been made in this direction. The times that coatings will protect refractory metals from oxidation under constant temperature conditions are indicated by the solid curves and under cyclic temperatures by the dashed curves. (See, for example, refs. 16 to 19.) Results are given for alloys of the four important refractory metals of interest, namely, tungsten, tantalum, molybdenum, and columbium. The curves represent a generally optimistic average of test information for several coatings including silicic, metallic or intermetallic, and ceramic types. With the exception of coatings for tungsten, several commercially available coatings will yield the type of results shown here. Coatings for tungsten are generally in the laboratory development stage at the present time.

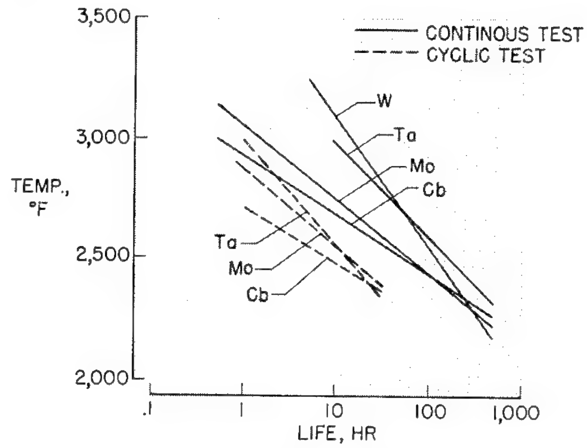

FIGURE 73–18.—Life of coated refractory metal sheet under continuous or cyclic temperatures.

These results indicate that present-day coatings can provide continuous protection of at least 1 hour at 3000° F to 100 hours at 2500° F and that an order of magnitude or greater decrease in coating life is obtained under cyclic exposure conditions. The serious degradation that is obtained under cyclic temperature exposure has direct bearing on the reusability of refractory metal components in aerospace vehicles. Further efforts to improve coating performance, particularly under cyclic temperatures, appear to be warranted.

One item of concern regarding utilization of coatings on refractory metals is based on the fact that the life of large complex structural components will generally be less than the life obtained from small materials coupons. This problem is indicated in figure 73–19. Figure 73–19 indicates the test temperatures and corresponding life for coated molybdenum coupons and coated corrugated-core sandwich panels.

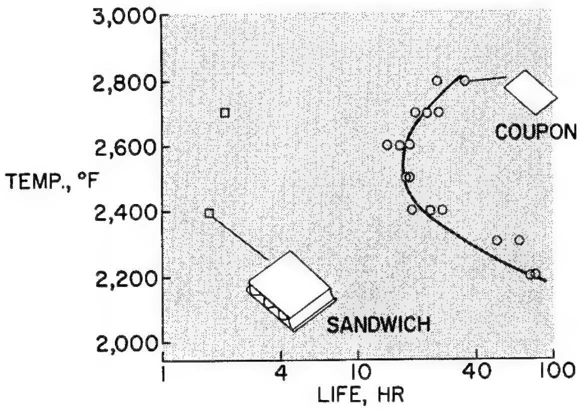

FIGURE 73-19.—Comparison between life of coated molybdenum coupons and life of coated molybdenum sandwich panels.

(See ref. 20.) The coating is a commercially available disilicide type. Life is defined as the time at test temperature during which the coating protected the metal with no measurable evidence of oxidation. The circle symbols indicate test results from small square sheet coupons tested continuously in slowly moving air in an electrically heated furnace. In the temperature range from 2400° F to 2700° F, a coating life of approximately 20 hours was obtained. The square test symbols indicate the life of two coated structural specimens under similar test conditions. The structural specimens consisted of corrugated-core sandwich plates. The difference in lifetime may be attributed to the difficulty of coating the sharp corners and recessed areas and to nonuniform expansion of various parts that may cause defects in the coating.

Several other factors have an important bearing on the performance and reliability of coated refractory metals. These include protection afforded by the coating under dynamic airflow, the performance of the coating under low pressure simulating high-altitude environment accompanied by high temperatures, and a better understanding of the protective mechanism and the modes of failure of the various types of coatings.

CONCLUDING REMARKS

To conclude this presentation, several research areas of particular importance to winged aerospace vehicles are noted and special problems in these areas that require further work are indicated. Under structural concepts, further attention should be devoted to formulation of new concepts and to analytical study of structural systems that incorporate thermal-protection and load-carrying functions into a single component. Further study of methods for application of transpiration cooling to winged aerospace vehicles should also be pursued. With reference to aerothermoelasticity, analytical studies are required to bring about a better understanding of flutter of orthotropic panels under aerodynamic heating. Two problems are noted under acoustic fatigue. These include characterization of boundary-layer noise at hypersonic speeds and development of approaches for establishing structural response and fatigue life. Under materials, the development of methods for application of notch-strength information to vehicles design, the improvement of coatings, and better understanding of protective mechanism and modes of failure of the coatings are of particular importance.

REFERENCES

1. MELLINGER, GEORGE R.: The X-15. Aerospace Engineering, vol. 20, no. 8, Aug. 1961, pp. 12-13, 26, 28-30, 32, 34-36, 38.
2. YOLER, YUSUF A.: Dyna-Soar—A Review of the Technology. Aerospace Engineering, vol. 20, no. 8, Aug. 1961, pp. 8-9, 56-67.
3. FRICK, C. W., and STRAND, T.: Recoverable Air-Breathing Boosters—Analysis of Their Potentialities. Aerospace Engineering, vol. 20, no. 2, Feb. 1961, pp. 22-23, 66-70.
4. GARRICK I. E., and CUNNINGHAM, HERBERT J.: Problems and Developments in Aerothermoelasticity. Proceedings of Symposium on Aerothermoelasticity, ASD Tech. Rep. 61-645, U.S. Air Force, 1961, pp. 12-60.
5. HELDENFELS, RICHARD R.: Frontiers of Flight Structures Design. Aeronautics and Astronautics, Nicholas John Hoff and Walter Guido Vincenti, eds., AFOSR TR 59-108, Pergamon Press, Inc. (New York), 1960, pp. 29-51.
6. GLASER, PETER E., ed.: Aerodynamically Heated Structures. Prentice-Hall, Inc., 1962.

7. PRIDE, RICHARD A., ROYSTER, DICK M., and HELMS, BOBBIE F.: Experimental Study of a Hot Structure for a Reentry Vehicle. NASA TM X-314, 1960.
8. ANDERSON, MELVIN S., and STROUD, C. W.: Experimental Observations of Aerodynamic and Heating Tests on Insulating Heat Shields. NASA TN D-1237, 1962.
9. GUY, LAWRENCE D., and DIXON, SIDNEY C.: A Critical Review of Experiment and Theory for Flutter of Aerodynamically Heated Panels. Presented at Symposium on Dynamics of Manned Lifting Planetary Entry (Philadelphia, Pa.), Oct. 29–31, 1962.
10. HUBBARD, HARVEY H., and MAGLIERI, DOMENIC J.: Supersonic Transport Noise Problems. Presented to International Air Transport Association (Montreal, Canada), Apr. 17–28, 1961.
11. HILTON, DAVID A., MAYES, WILLIAM H., and HUBBARD, HARVEY H.: Noise Considerations for Manned Reentry Vehicles. NASA TN D-450, 1960.
12. EDGE, PHILIP M., JR.: Acoustic Fatigue Tests Relating to the Design of Structures for Elevated Temperatures. Presented at ONR/AIA Symposium on Structural Dynamics of High Speed Flight (Los Angeles, Calif.), Apr. 24–26, 1961.
13. SACHS, G., and PRAY, R. FORD, III, eds.: Air Weapons Materials Applications Handbook Metals and Alloys. ARDC TR 59-66, U.S. Air Force, Dec. 1959.
14. WEISS, V., SELL, R., and CHAVE, C.: Material Evaluation for a Supersonic Transport Plane. Rep. No. MET. E. 873-626-F (Contract No. NASr-43), Syracuse Univ. Res. Inst., June 1962.
15. NEFF, C. W., FRANK, R. G., and LUFT, L.: Refractory Metals Structural Development Program. Vol. II—Refractory Alloy and Coating Development. ASD Tech. Rep. 61-392, U.S. Air Force, Oct. 1961.
16. KRIER, C. A.: Coatings for the Protection of Refractory Metals From Oxidation. DMIC Rep. No. 162, Battelle Memorial Inst., Nov. 24, 1961.
17. NICHOLAS, M. G., PRANATIS, A. L., DICKINSON, C. D., and WHITMAN, C. I.: The Analysis of the Basic Factors Involved in the Protection of Tungsten Against Oxidation. ASD-TDR-62-205, U.S. Air Force, June 1962.
18. LAWTHERS, DEAN D., and SAMA, L.: High Temperature Oxidation Resistant Coatings for Tantalum Base Alloys. ASD Tech. Rep. 61-233 (Contract AF 33(616)-7462), U.S. Air Force, 1961.
19. RUMMLER, D. R., STEIN, B. A., and PRIDE, R. A.: Preliminary Results of a Comparative Study of Several Commercially Available Oxidation Resistant Coatings on Mo-0.5 Ti Alloy Sheet. Presented at Sixth Meeting of the Refractory Composites Working Group (Dayton, Ohio), June 16–19, 1962.
20. MATHAUSER, ELDON E., STEIN, BLAND A., and RUMMLER, DONALD R.: Investigation of Problems Associated With the Use of Alloyed Molybdenum Sheet in Structures at Elevated Temperatures. NASA TN D-447, 1960.

Research, Design Considerations, and Technological Problems of Structures for Planetary Entry Vehicles

By Roger A. Anderson

ROGER A. ANDERSON, *Assistant Chief, Structures Research Division, NASA Langley Research Center, received his Bachelor of Science degree in Civil Engineering from Northwestern University in 1944.*

Anderson joined the Langley staff as a structural engineer in June 1944. With the emergence of reentry as a dominant problem in space structures and materials, Anderson has taken special interest in the problems of thermal protection systems ranging from analysis and evaluation of present capabilities to projected requirements for accomplishment of future manned and unmanned space missions. Anderson has served as a member of the evaluation boards for the Dyna-Soar glider, the Mercury spacecraft, and the Apollo System. He has served on several technical committees at Langley and other national organizations and currently serves on the Structures and Materials Committee of the American Rocket Society. He is the author of numerous technical papers in the field of aerospace structures.

SUMMARY

The technology for structural design of manned and unmanned planetary-entry vehicles is reviewed. Emphasis is placed on the important features of these vehicles—the thermal shield and the landing system. Basic structural and material concepts are discussed in the light of applicable environmental conditions, and areas for further research are suggested.

INTRODUCTION

The technology for structural design of space vehicles whose mission includes a successful high-speed entry into a planet's atmosphere has had a relatively short but eventful history of development. Knowledge has accumulated rapidly through the practical experience gained in the design and successful flights of vehicles such as the Mercury spacecraft and a number of smaller vehicles which preceded it. Flight requirements continue to expand in the direction of higher speeds and longer and more complex missions; consequently, new materials and concepts of construction are still needed.

In this review the primary emphasis will be placed on the unique feature of the entry vehicle—the thermal shield and its integration with structure—inasmuch as it accounts for an important fraction of the weight and of the problems in vehicle design. Because entry is not completed for most vehicles until a soft landing on a planet's surface has been made, current thinking regarding final letdown and impact will also be briefly reviewed.

SYMBOLS

A	frontal area of vehicle
C_D	drag coefficient
g_E	acceleration due to Earth's gravity
q	heating rate
Q	heat load per unit area
t	time
W	total weight or weight per unit area
W_{SYS}	system weight
W_{VEH}	vehicle weight
ρ	density

GENERAL DESIGN CONSIDERATIONS

Entry vehicles are conveniently divided into two basic types—the unmanned vehicle designed for a specific research purpose, and the considerably larger vehicle utilized for manned missions. The structural approach for each class varies because of differences in size, shape, and degree to which the internal environment needs to be controlled.

Features of the unmanned class are shown in figure 74–1. Characteristically, they are ballistic bodies of relatively simple shape. The primary structure usually conforms to the aerodynamic outline and a layer of ablative material is bonded directly to it. In this manner internal volume is maximized and structural weight is held to a minimum. The principal structural complication is in the form of sensor and telemeter antenna installations. Windows which maintain transparency at specific optical and radio wave frequencies must be installed and are not always located in regions of low heat transfer. Such installations give rise to localized heating problems and require detailed thermal and stress analysis.

With the vehicle for manned missions (fig. 74–2), a much wider variation in aerodynamic configuration is encountered. They include the ballistic as well as the lifting shapes which provide a wider entry corridor and a horizontal-landing capability. For this class of vehicles the primary pressure shell forming the cabin does not differ substantially from current aero-

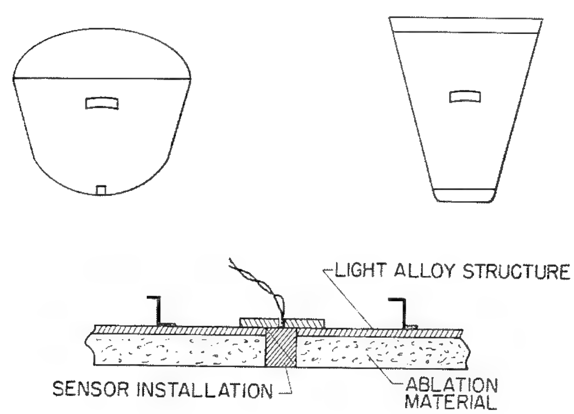

FIGURE 74–1.—Construction of unmanned entry vehicle.

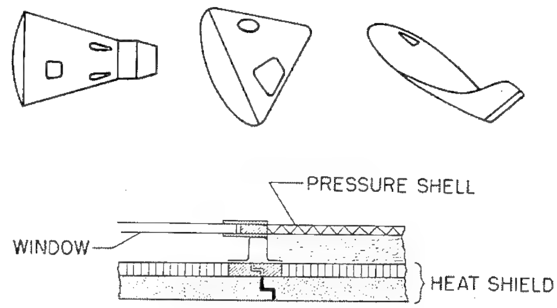

FIGURE 74–2.—Construction of manned entry vehicle.

nautical practice except for the precautions taken to maintain leak tightness. It usually does not conform to the external lines and is protected against entry heating by a separate structural component commonly referred to as a heat shield. The space between the cabin and the heat shield is occupied by insulation, connecting structure, and items of equipment which do not require storage in the controlled environment of the pressure cabin. The hatch and window openings in the cabin require doors in the heat shield. These cutouts in turn must be fitted with hatches which can be opened and closed during a mission. The associated interruptions in shield continuity are of concern during the entry phase. In addition, large sections of the shield may serve as a part of the landing-impact absorption system. Because of such features the heat shield can account for more than one-half the total structural weight of the vehicle.

In the selection of materials and design criteria for these structures, consideration is given to a wide spectrum of environmental conditions from initial assembly to final impact. These considerations are illustrated in figure 74–3. Assembly and disassembly operations must be considered in the basic design concept because of the demonstrated need for ease of access through the structure for repair and replacement of internal components. Repair of damage associated with ground-handling operations is a consideration in the choice of materials, especially those used for the heat shield.

The launch phase subjects the structure to a variety of vibratory and acoustic loadings. A review of these loadings may be found in ref-

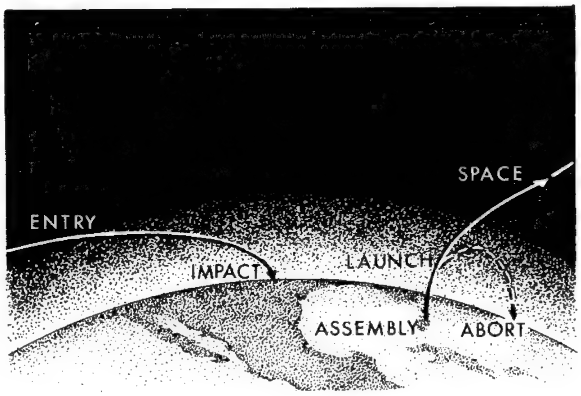

FIGURE 74-3.—Vehicle design considerations.

erence 1. The critical design values of aerodynamic load are likely to be encountered during launch. This is particularly true for manned vehicles which are designed for safe abort during any portion of the launch phase. Possible degradation of the surface of the heat shield due to heating during ascent requires attention.

An exposure to space environment for extended periods places a number of constraints on material selection. (See ref. 2.) Of most concern is the response of the heat shield to micrometeoroid impact and its subsequent performance during entry. At least for missions of short duration, the heat shield is called upon to serve as the meteoroid bumper and its construction must reflect this requirement. For longer missions, an additional consideration in selection of materials will be the shielding they afford against ionizing radiation.

The heat shield performs its primary design function during the entry phase. The severity and duration of heating and loading varies widely with vehicle type and trajectory (see ref. 3); consequently, a large number of material and structural concepts have evolved (refs. 4, 5, and 6). Proper selection of materials and prediction of their performance as mission times and entry speeds increase is a large and challenging research task.

After conclusion of the high-heating and deceleration phase, vehicle terminal velocity is generally too high for a survivable impact on a planet's surface. Loads associated with deployment of a suitable letdown system and support of an impact energy absorber contribute significantly to structural weight and to final structural arrangement.

Integration of the design inputs arising from this sequence of environments has resulted in structural weights that currently range from 30 to 55 percent of vehicle gross weight depending on the mission. These percentages are approximately twice those associated with aeronautical structures and primarily reflect the penalty of the thermal shield required during the entry phase.

HEAT-SHIELD PERFORMANCE

A broad picture of the role that the thermal shield plays in determining the feasibility of future entry vehicles is presented in figure 74-4. Vehicle kinetic energy, heat-shield capability, and vehicle heat load, all expressed in Btu/lb, are shown as a function of entry velocity. The range of velocity shown must be considered if exploration of nearby planets is to be carried out. (See ref. 7.) Of the tens of thousands of Btu's of kinetic energy possessed by each pound of the entering vehicle, the major portion is dissipated in heating the atmosphere with only a small fraction returning as a heat load on the vehicle surface. At the lower velocities heat transfer to the vehicle is primarily by convection, whereas at the higher velocities radiative transfer from the highly heated shock wave contributes importantly. (See refs. 8, 9, and 10.)

The width of the heat-load band at a given velocity reflects differences in vehicle configuration and entry trajectory. Vehicles entering

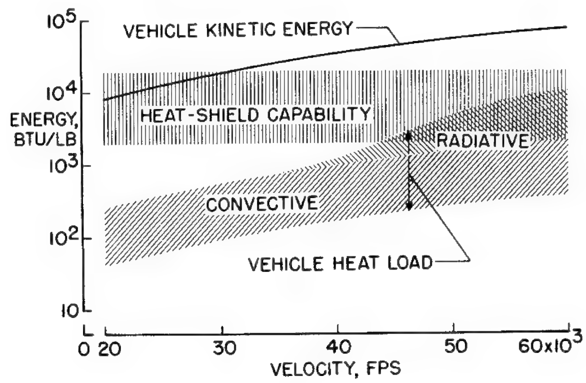

FIGURE 74-4.—Kinetic-energy dissipation.

on ballistic trajectories encounter heat loads near the lower edge of the band, whereas vehicles flying lifting trajectories move higher in the band. Detailed knowledge of the heat load to be encountered by a given vehicle at the higher speeds is admittedly sketchy because of currently unresolved uncertainties in heat-transfer mechanisms.

Heat-shield capability can be represented by a broad band encompassing the range from 2,000 to 20,000 Btu/lb. That is, with currently known materials, each pound of heat shield can be expected to dispose of a certain amount of heat energy within this range while maintaining an acceptably cool vehicle interior for the duration of the entry maneuver. The diminishing separation between the bands of heat-shield capability and vehicle heat load suggests an increasing degree of difficulty in preserving a useful payload margin as entry speed increases. Observations of meteors in the Earth's atmosphere reveal a greatly diminished chance for survival at speeds in excess of 55,000 fps. (See ref. 7.) Clearly, at the higher speeds, vehicles designed for minimum total heat transfer and utilizing the most advanced heat-shield technology will be required if reasonable payload margins are to be preserved.

Because of wide variations in the time histories of heat transfer to various vehicle types, it may be helpful to examine figure 74–5. The stagnation-area heating histories shown are typical for a research vehicle entering the Earth's atmosphere on a fairly steep ballistic trajectory and for manned vehicles making

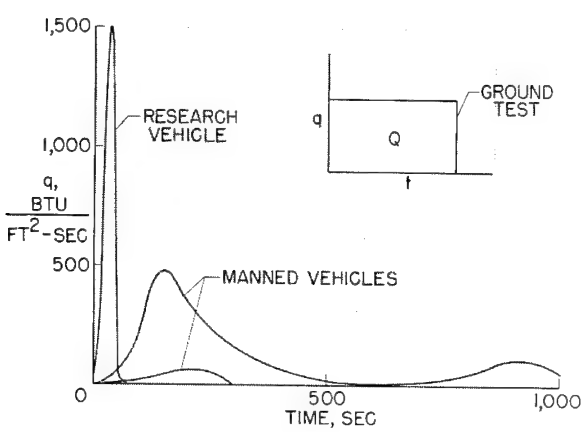

FIGURE 74–5.—Typical heating histories.

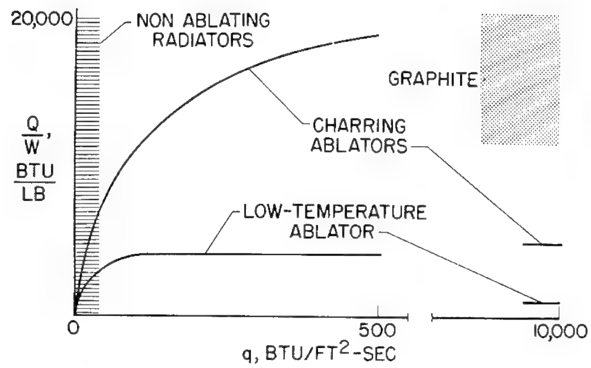

FIGURE 74–6.—Relative performance of thermal shields.

shallow-angle entries at orbital and escape velocity. The associated differences in heating rate and heating time have a substantial influence on the choice of shield material.

In the process of screening applicable materials and shield concepts for a given vehicle, a constant heating-rate pulse is usually employed. A desired constant total heat input Q can be obtained by varying the heating rate q and time t. The weight of material required to dispose of a given value of Q without significant penetration of heat to the shield interior side becomes a measure of shield performance.

The relative performance of several shield materials (at constant stream enthalpy) is shown in figure 74–6. An inverse measure of shield weight Q/W is plotted as a function of the imposed heating rate q. A break in scale is introduced to permit inclusion of the extreme heating rates associated with the higher speed entry problem.

At heating rates below about 40 Btu/ft^2-sec, the current limit of serviceability for nonablating metallic surfaces, an insulating shield which disposes of heat by reradiation provides the best performance. (See ref. 11.) Because of fixed items of weight associated with construction of metallic-surfaced heat shields, the efficiency of the system depends to a large extent upon the total heat load. In vehicle areas where low heating rates permit utilization of this type of shield, a performance of the order of 20,000 Btu/lb can be achieved in a gliding entry of long duration.

In the intermediate heating-rate range, a class of materials known as charring ablators

has proven to provide a highly efficient thermal shield. (See refs. 12 and 13.) The improvement in their performance over a low-temperature ablator, such as Teflon, stems from the fact that their surfaces are forced to a high temperature by the insulating char layer formed during material pyrolysis. Thus, in addition to benefiting from the transpiration cooling provided by the gaseous products of pyrolysis, they dispose of a substantial fraction of the imposed heat load by reradiation from the hot surface.

At extreme values of heating rates, a degradation in performance is estimated for both the charring and low-temperature ablators as shown by the extension of their respective curves in figure 74–6. A qualitative explanation for this reduction is that, at the entry conditions which generate these high rates, a large fraction of the heating is presumed to be by radiation from the incandescent gas cap surrounding the vehicle. Under these conditions transpiration is less effective as a cooling mechanism. (See ref. 14.) In addition, high aerodynamic shear forces and thermal stresses may inhibit buildup of an insulative char layer on the charring ablators and thereby lead to mass loss rates more comparable to those for the low-temperature ablator.

A promising candidate material for the high-heating-rate regime is graphite. (See ref. 15.) Its high latent heat of vaporization can be used to advantage without too great concern for its relatively high thermal conductivity which hinders application at lower heating rates. A number of uncertainties remain regarding the performance of graphite under high rates of radiant and convective heating, among which is possible mechanical removal of material by spalling from thermal stresses associated with extremely steep thermal gradients. Data on the actual values of the heat of vaporization over the applicable ranges of temperature and pressure also appear to be incomplete. (An analysis of the available data is given in ref. 16.) For these reasons, the performance of graphite can only be estimated and is indicated by the shaded area shown in figure 74–6.

A particular range of heating rates in which marked advances in heat-shield performance

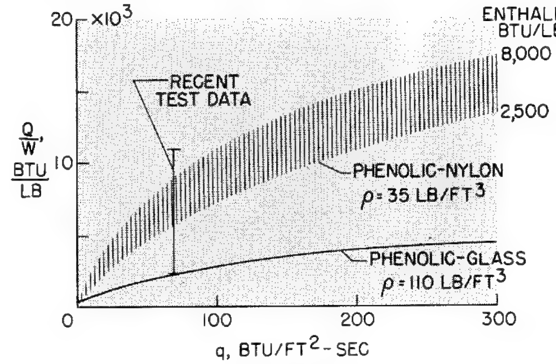

FIGURE 74–7.—Performance of charring ablators.

have been obtained in recent research is at the low end of the scale where conduction of heat through the shield to the interior is primarily responsible for the indicated dropoff in performance. This area is shown in more detail in figure 74–7. Available test data for low-density phenolic-nylon material were used to construct the indicated band. A sensitivity to stream enthalpy is noted with this charring ablator because of the high degree of vaporization obtained with nylon.

In contrast, a high-density phenolic-glass shield showed negligible enthalpy sensitivity in the same tests and provided markedly shorter protection times because of its relatively high thermal conductivity. Recent data gathered at one heating rate have revealed low-density shield compositions which show substantially higher performance. There is no reason to believe that an end point in improvement has yet been reached. In this connection, it should be noted that large surface areas of manned entry vehicles are subject to heating rates in this low range where shielding performance depends greatly on the material's ability to perform as an insulator.

A cross-sectional view of a high-performance shield is provided in figure 74–8. Here the ablative component of the shield is seen to possess a cellular structure which provides a high resistance to heat flow through the thickness. Materials of this type have low strength and stiffness and are therefore confined in a fiberglass honeycomb matrix for local reinforcement. Adequate bending stiffness is provided by attachment to a conventional honeycomb

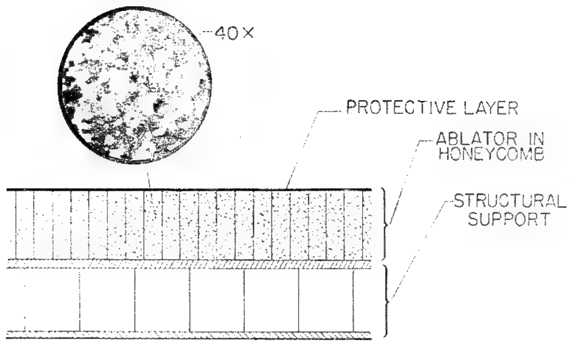

FIGURE 74–8.—Advanced shield design (low heating rates).

sandwich panel. The panel material and gage may be determined by the meteoroid impact problem as well as by stiffness or strength criteria. The indicated protective layer at the surface may be necessary to provide resistance to abrasion during ground handling and launch, and may be required in space to obtain desired values of reflectivity and emissivity. Investigation of variations of the general design concept illustrated in figure 74–8 is a subject of current research.

GROUND RESEARCH

The bulk of ground research performed on heat-shield structures to date has of necessity been rather narrowly oriented to direct support of specific vehicle projects. The situation is changing, but with few exceptions little data can yet be assembled from the open literature for general engineering design use. The type of work underway, however, is of interest, and some of it is indicated in figure 74–9.

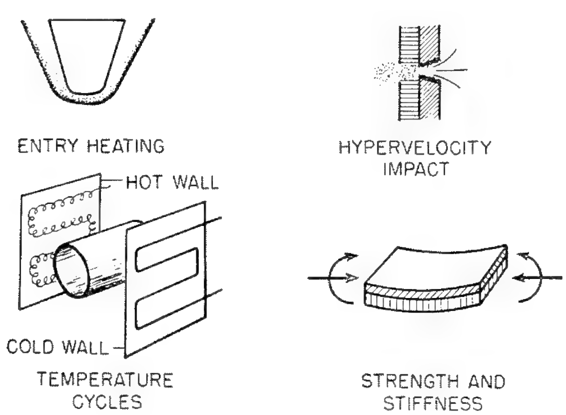

FIGURE 74–9.—Ground research.

Numerous organizations are conducting tests of materials and small structural samples in simulated entry environments. The electric arc-heated air jet in the power range of 1 to 10 megawatts is the principal facility used for this simulation. Numerous problems remain in developing this facility to its full capability, but steady advances are being made in the areas of increased stream enthalpy, Mach number, running time, model size, and control of stream chemistry. Facilities capable of combined convective and radiative heating simulation over certain ranges of heating rates are available at NASA Ames and Langley Research Centers. (See ref. 17.)

Space environmental tests in which fabricated sections of heat-shield structure are subjected to the temperature distributions and cycles expected during a space journey are being made. Radial and circumferential thermal gradients are varied to expose areas of failure due to thermal stresses. Adequate stress analysis is usually hindered by a lack of physical-property data for new shield materials and by the difficulty in accurately specifying the restraints offered by attachments between structural elements.

Some work has been accomplished on the response of shield structures to hypervelocity impact. Such tests need to be carried out at various temperature levels because of marked variations in the properties of polymeric materials with temperature. Ground facilities for this purpose are still limited in the attainable impact velocity and maximum particle size.

Inasmuch as the heat-shield structure can be required to transmit loads over considerable spans, the usual strength and stiffness tests and analysis must be performed. Again, the temperature level at which tests are carried out is important.

In addition to the work illustrated, there are numerous research investigations (see refs. 18 and 19 as examples) concerned with obtaining a basic understanding of these composite materials in the many environments of concern. These investigations, however, still leave the designer short of a final proof test on a full-scale structure with rather complete environmental simulation. Because of test-facility limitations,

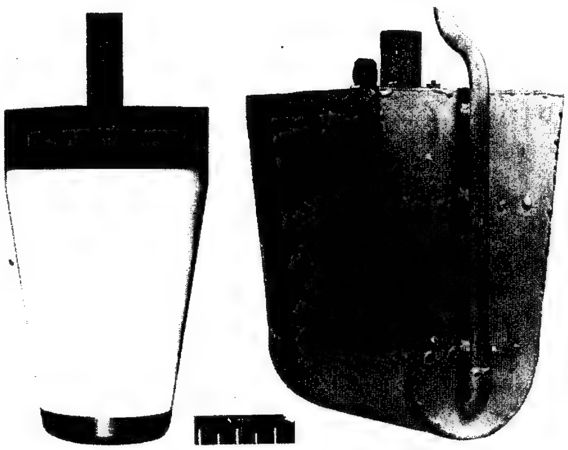

FIGURE 74-10.—Structural test specimens.

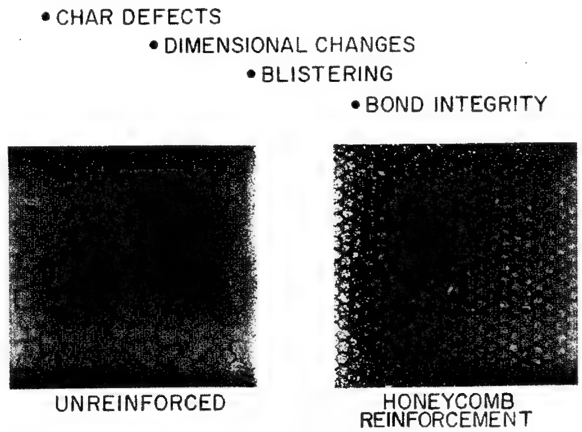

FIGURE 74-11.—Low-heating-rate problems.

completely satisfactory proof tests on the ground cannot yet be made, but a step in this direction has been taken in tests of small structural models in arc-jet facilities. Two such models are shown in figure 74-10.

The blunted cone is a one-third-scale model of a flight research payload. With this model the conical surface is the primary test area. This area is of sufficient size to study failure mechanisms associated with differential thermal expansion as well as the effect of discontinuities and joints in the ablative shield. The round-nose wedge is a water-cooled holder for a 5-inch-square test panel. The flat panel affords some economy in specimen preparation. Currently, such specimens are tested in a large-diameter subsonic arc jet.

Views of 5-inch-square specimens tested to determine performance of charring ablators at very low heating rates are shown in figure 74-11. Characteristic problems revealed are various forms of char defects, gross dimensional changes due to thermal expansion, formation of blisters during escape of pyrolysis products, and destruction of the bond between the ablative layer and its supporting structure prior to complete pyrolysis of the ablator. The samples displayed here illustrate the after-test appearance of two materials—one without a reinforcement, and one reinforced with a honeycomb. Among other benefits of reinforcement, it is seen that fissures in the char layer are confined to the honeycomb cell dimension.

Figure 74-12 shows typical results of tests designed to explore the effects of various types of discontinuities in shield materials. The result on the left illustrates the behavior of a ring of a noncharring low-temperature ablator inserted as an antenna window through a char-forming shield. The undercutting that was exhibited was considered undesirable in the full-scale flight vehicle, and a decision was made to use a heavier weight of the noncharring material for protection of the entire afterbody.

A pattern of holes similar to that shown on the face of the smaller specimen in figure 74-12 can arise from a need for electrical connections through the heat shield. Limited tests on a charring ablator have indicated that small holes are permissible, at least when located in areas

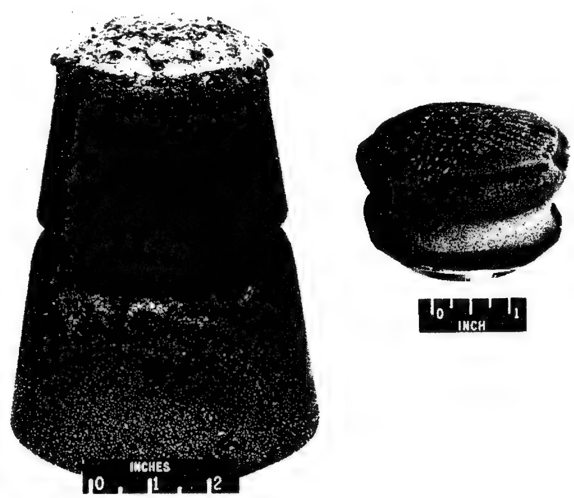

FIGURE 74-12.—Shield discontinuities.

of low dynamic pressure and shear force. However, the general problem of defining the tolerance limits for a given shield material to discontinuities of various types, including damage caused by micrometeoroid impact, is one warranting much more detailed investigation.

FINAL LETDOWN SYSTEMS

After an entry vehicle has passed through the primary deceleration and heating phase and a speed near the terminal value in a particular atmosphere has been reached, there remains the problem of decelerating to a safe touchdown speed. The horizontal landing mode, of course, implies an aerodynamically suitable design and some preparation of the landing site. For arbitrary landing terrain conditions, and for the unmanned class of vehicles, a vertical descent will continue to find favor. For this type of descent both the parachute and the rocket landing systems have been studied, and a comparison of their weights is shown in figure 74–13. Weight of these systems as a percentage of vehicle weight is given as a function of planetary characteristics which determine the terminal velocity of freely falling bodies. Values of this ratio or Venus and Mars are indicated along with the value for Earth. The "greenhouse model" atmosphere (ref. 20) for Venus was chosen. A final impact velocity of 30 fps was assumed for this comparison.

Inasmuch as parachute-system weight (ref. 21) is not entirely independent of vehicle size and weight, a 7,000-pound vehicle was arbitrarily chosen for the calculation of parachute-system weight. As would be anticipated, parachute-system weight is highly sensitive to variations in planetary characteristics. Rocket-system weight depends in somewhat greater detail upon the exact kinetic and potential energy to be dissipated and the maximum deceleration level. These considerations lead to a weight band for vehicles lying within the specified limits of the aerodynamic drag parameter W/C_DA and subject to a maximum deceleration of 10 Earth g's.

The weight of letdown systems is seen to represent a significant percentage of vehicle weight on planets such as Earth and Mars. For planets like Mars with a low atmospheric density, it appears that a braking rocket could lead to the least weight system. For celestial bodies without an atmosphere, of course, it is the only choice.

After deceleration to 30 fps prior to contact, a formidable problem in landing-gear design still remains when large differences in surface terrain are considered. Variations in landing-gear geometry is a subject by itself and cannot be adequately treated here, but it may be instructive at least to look at the capability of those materials which either have been used, or have possibilities for use, as the energy-absorption medium in various gear designs. Such a comparison is presented in figure 74–14. (See refs. 22 to 25.)

Energy-dissipation capability is again presented as Btu/lb with the energy absorbed in

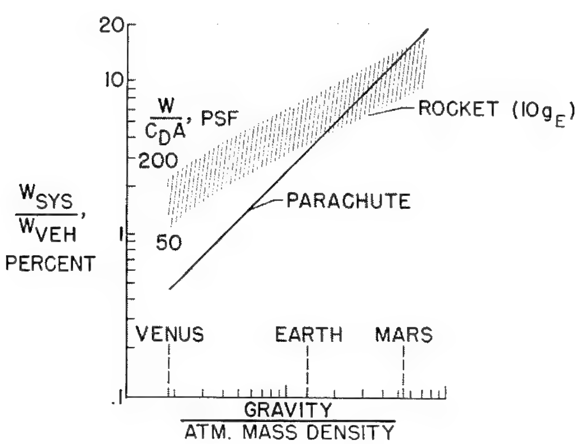

FIGURE 74–13.—Letdown system weight. Impact velocity, 30 fps.

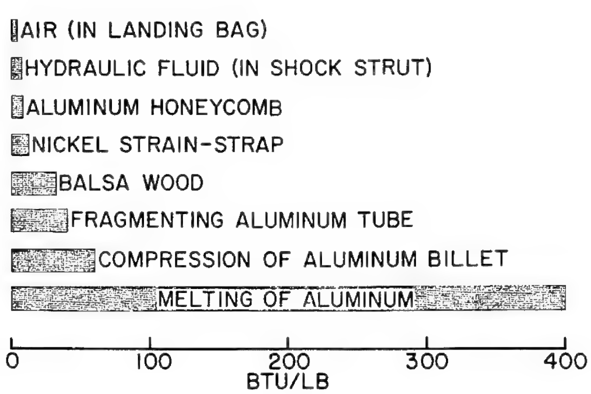

FIGURE 74–14.—Energy-dissipation capabilities of materials.

heating aluminum to its melting point used as a yardstick. The energy absorbed by the common working media, air and hydraulic fluids in their confining structures, is seen to be quite small in relation to the work done in crushing or deforming solid materials. Honeycomb, strain-straps, and balsa wood have already been incorporated in vehicle-impact absorption systems. The work done in fragmenting an aluminum tube begins to approach that done in straight compression of an aluminum billet, and offers controllable values of decelerating force. Simple devices which give controlled fragmentation at predictable force levels have been developed. In view of the disparity between current capability and that which may be achievable, further research on impact absorption appears to be warranted.

CONCLUDING REMARKS

For heat shields, new concepts in materials, fabrication process, and integration with structure are needed to cope with the wide variety of environmental conditions encountered in an extended flight mission. Ultimately, ease of refurbishment for successive missions will become an important requirement.

Along with advances in concepts more attention needs to be given to stress-analysis methods appropriate to shield materials and configurations. The problem becomes more difficult when thermal degradation of material properties accompanying the heating is included in the analysis.

Research on space environmental effects on a variety of materials has been proceeding for some time but little information is yet available on the materials of particular interest in heat-shield construction.

Response of materials to extreme rates of radiative heating needs to be explored in much greater detail. Also, shield design concepts which are effective in either reflecting or absorbing high radiant rates must be sought.

Testing methodology for heat shields is developing slowly. Research on techniques leading to reproducible and more generally usable engineering data are needed. The source of this problem probably can be traced to the fact that standardization of test methods is difficult in a technology with rapidly changing requirements.

With respect to landing systems, concepts other than some form of parachute may be appropriate if a letdown to the surface of planets with lower atmospheric density is to be made efficiently. The use of braking rockets appears promising for manned vehicles but would pose numerous problems in unmanned missions. For these missions, more promise may lie in the development of highly efficient techniques for absorbing the energy of higher velocity landing impacts.

REFERENCES

1. Runyan, Harry L., and Leonard, Robert W.: Research, Design Considerations, and Technological Problems of Structures for Launch Vehicles. NASA-University Conference on the Science and Technology of Space Exploration, vol. 2, 1962, pp. 487–498.
2. Jaffe, Leonard D., and Rittenhouse, John B.: Behaviour of Materials in Space Environments. ARS Jour., vol. 32, no. 3, Mar. 1962, pp. 320–346.
3. Love, Eugene S.: Reentry Vehicles: General Concepts and Operational Modes. Reentry Dynamics. Bull. of Virginia Polytechnic Inst., Eng. Exp. Station Ser. No. 150, vol. LV, no. 10, Aug. 1962, pp. 16–52.
4. Swann, Robert T.: Composite Thermal Protection Systems for Manned Re-Entry Vehicles. ARS Jour., vol. 32, no. 2, Feb. 1962, pp. 221–226.
5. Glaser, Peter E., ed.: Aerodynamically Heated Structures. Prentice-Hall, Inc., 1962.
6. Anderson, Roger A.: Thermal Protection Systems and Structures for Reentry Vehicles. Reentry Dynamics. Bull. of Virginia Polytechnic Inst., Eng. Exp. Station Ser. No. 150, vol. LV, no. 10, Aug. 1962, pp. 207–230.
7. Riddell, Frederick R., and Winkler, Howard B.: Meteorites and Re-Entry of Space Vehicles at Meteor Velocities. ARS Jour., vol. 32, no. 10, Oct. 1962, pp. 1523–1530.
8. Teare, J. D., Georgiev, S., and Allen, R. A.: Radiation From the Non-Equilibrium Shock Front. Res. Rep. 112 (AFCRL 937), Avco-Everett Res. Lab., Oct. 1961.

9. ROSE, P. H.: Radiation and Ionization Problems in Re-Entry. Reentry Dynamics. Bull. of Virginia Polytechnic Inst., Eng. Exp. Station Ser. No. 150, vol. LV, no. 10, Aug. 1962, pp. 156–206.
10. SCALA, SINCLAIRE M., and WARREN, WALTER R.: Hypervelocity Stagnation Point Heat Transfer. ARS Jour. (Tech Notes), vol. 32, no. 1, Jan. 1962, pp. 101–102.
11. ANDERSON, ROGER A., and SWANN, ROBERT T.: Structures for Reentry Heating. NASA TM X–313, 1960.
12. WADLIN, KENNETH L., and KOTANCHIK, JOSEPH N.: The Use of Ablators for Achieving Protection Against High Thermal Flux. [Preprint] 417C, Soc. Automotive Eng., Oct. 1961.
13. BROOKS, WILLIAM A., JR., SWANN, ROBERT T., and WADLIN, KENNETH L.: Thermal Protection for Spacecraft Entering at Escape Velocity. [Preprint] 513F, Soc. Automotive Eng., Apr. 1962.
14. SWANN, ROBERT T.: Effect of Thermal Radiation From a Hot Gas Layer on Heat of Ablation. Jour. Aerospace Sci. (Readers' Forum), vol. 28, no. 7, July 1961, pp. 582–583.
15. NOLAN, EDWARD J., and SCALA, SINCLAIRE M.: Aerothermodynamic Behaviour of Pyrolytic Graphite During Sustained Hypersonic Flight. ARS Jour., vol. 32, no. 1, Jan. 1962, pp. 26–35.
16. GLOCKER, GEORGE: Heat of Sublimation of Graphite and the Composition of Carbon Vapor. Jour. Chem. Phys., vol. 22, no. 2, Feb. 1954, pp. 159–161.
17. HELDENFELS, R. R.: Ground Facilities for Testing Reentry Structures and Materials. Reentry Dynamics. Bull. of Virginia Polytechnic Inst., Eng. Exp. Station Ser. No. 150, vol. LV, no. 10, Aug. 1962, pp. 314–338.
18. SCALA, SINCLAIRE M., and GILBERT, LEON M.: Thermal Degradation of a Char-Forming Plastic During Hypersonic Flight. ARS Jour., vol. 32, no. 6, June 1962, pp. 917–924.
19. STEG, L., and LEW H.: Hypersonic Ablation. Tech. Inf. Series No. R62SD55—Class I, Missile and Space Vehicle Dept., Gen. Elec. Co., May 1962.
20. KELLOGG, WILLIAM W., and SAGAN, CARL: The Atmospheres of Mars and Venus. Pub. 944, Nat. Res. Council, Nat. Aca. Sci., 1961.
21. PARACHUTE BRANCH, DIRECTORATE OF DEVELOPMENT: United States Air Force Parachute Handbook. WADC Tech. Rep. 55–265, ASTIA Doc. No. AD 118036, U.S. Air Force, Dec. 1956.
22. BROOKS, GEORGE W., and CARDEN, HUEY D.: A Versatile Drop Test Procedure for the Simulation of Impact Environments. Noise Control Shock and Vibration, vol. 7, no. 5, Sept.-Oct. 1961, pp. 4–8.
23. MCGEHEE, JOHN R.: A Preliminary Experimental Investigation of an Energy-Absorption Process Employing Frangible Metal Tubing. NASA TN D–1477, 1962.
24. FISHER, LLOYD J., JR.: Landing-Impact-Dissipation Systems. NASA TN D–975, 1961.
25. ESGAR, JACK B.: Survey of Energy-Absorption Devices for Soft Landing of Space Vehicles. NASA TN D–1308, 1962.

Research, Design Considerations, and Technological Problems of Structures for Spacecraft

By George W. Brooks

DR. GEORGE W. BROOKS, *Head, Vibration and Dynamics Branch, NASA Langley Research Center, completed his undergraduate and graduate work at Princeton University. He received his Bachelor of Science in Engineering in 1947, his Master of Science in Engineering in 1949, and his Ph D. in 1962. He is an instructor in advanced mathematics, teaching in the graduate study program conducted by Langley.*

Since joining the Langley staff in March 1949, he has specialized in helicopter dynamics, vibration analysis, dynamic modeling, spacecraft environments, planetology, and spacecraft design. Dr. Brooks supervised the design and research of the first flyable model for detailed dynamics studies of helicopters and has performed basic research in several areas of applied mechanics. His designs and concepts for a lunar and planetary gravitational simulator for impact research and a penetrometer system for measuring the hardness of the lunar and planetary surfaces are now under development. He is the author or co-author of numerous NASA publications on a variety of subjects in applied mechanics. He is a member of Phi Beta Kappa and RESA.

SUMMARY

The factors which influence the selection of the configuration and design features of spacecraft are reviewed. The multiplicity of configurations which result for the various mission objectives are exemplified by selected vehicles representative of compact, deployable, and inflatable structures. Problems unique to the design of these configuration types and general problems associated with the launch environment and space hazards such as vibrations, micrometeoroids, and thermal balance are discussed. The paper concludes with a discussion of techniques for achieving sterilization, and summarizes the problem areas where further research appears timely and appropriate.

INTRODUCTION

During the past 5 years great strides have been made in space flight, and to date nearly 100 spacecraft have been placed into orbit. The spacecraft launched during these flights varied substantially in mission, configuration, and size. All of them, however, had a common purpose—to furnish more and better information on the nature of the earth, the extraterrestrial bodies which surround it, and the hostile regions of space in between.

Another thing in common among all these spacecraft is the fact that they represent the state of the art in man's capability to build efficient lightweight manned and unmanned structures which have a high probability of withstanding the launch environment and yielding useful scientific data. It is the purpose of this paper to summarize this state of the art by reviewing some of the more important factors which influence the selection of spacecraft configurations and their structures, and to indicate problem areas in need of further study.

FACTORS WHICH INFLUENCE THE SELECTION OF SPACECRAFT CONFIGURATIONS

The primary factor in the selection of the configuration of a spacecraft is its mission, and the complexity of the mission usually dictates the complexity of the spacecraft. As an example, Echo I, the 100-foot-diameter balloon shown in figure 75–1, is relatively simple since it was designed primarily to serve as a passive communications satellite and therefore needed only to provide a reflective surface for radio waves. The balloon was constructed of a thin Mylar film coated with vapor-deposited aluminum. It was launched on August 12, 1960, and is still in orbit. During launch it was packaged in a sphere which had a diameter of 28 inches.

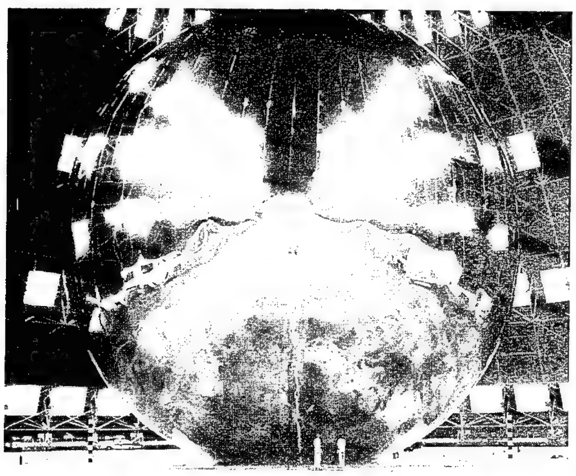

FIGURE 75–1.—Echo I (100-foot-diameter Mylar balloon).

The Apollo lunar excursion module, illustrated by the mockup shown in figure 75–2, is perhaps the best example of a complex spacecraft. A vehicle such as this must provide man with transportation to and from the lunar surface. Consequently it must incorporate the necessary life support systems to protect him from the extreme vacuum and temperature environment, and it must be designed to land and take off from a surface having poorly defined properties. In the latter respect, the design of the landing gear is a critical factor.

There are many other factors which have great influence on the selection of the configura-

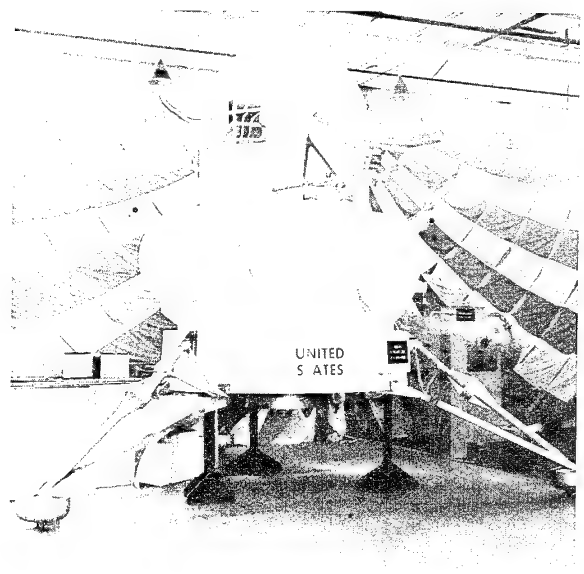

FIGURE 75–2.—Apollo lunar excursion module.

tion, such as launch-vehicle capability, onboard power requirements, communication requirements, and thermal protection for those spacecraft which are designed to reenter the earth's atmosphere.

MULTIPLICITY OF CONFIGURATIONS

The aforementioned requirements as well as the designer's preference result in a host of spacecraft configurations. Each of these configurations has its own advantages and inherent problem areas. It is possible, however, to classify spacecraft as they now exist into three rather broad types: compact, deployable, and inflatable. An attempt will be made in the following paragraphs to point out some of the pertinent characteristics and problem areas of each type.

Compact Spacecraft

It is possible to design many spacecraft as compact units. Examples of such vehicles are Vanguard, Explorer, Tiros, and the Telstar spacecraft shown in figure 75–3. From the dynamicist's viewpoint, such designs are highly desirable because it is much easier to control their structural response during the launch phase.

One of the more difficult problems with compact spacecraft is the provision of adequate

power in the allotted space for long-term operation of scientific instruments. Another important factor is thermal balance.

Deployable Spacecraft

The term "deployable spacecraft," as used herein, denotes those whose major components remain folded or constrained during launching and then are deployed to enable the spacecraft to perform its mission. There is little doubt that this class of vehicles represents those which have both the greatest versatility and the most difficult design problems. The Surveyor spacecraft shown in figure 75-4 is a typical example.

A brief look at such a spacecraft readily reveals a complex structure which consists of a combination of trusses, panels, hinges, plates, and so forth, and which is surely unlike any conventional airborne vehicle. In order to analyze such a structure to obtain its static and dynamic stresses and motions, one must resort to the fundamental concepts and develop the theory for each such vehicle. It is apparent

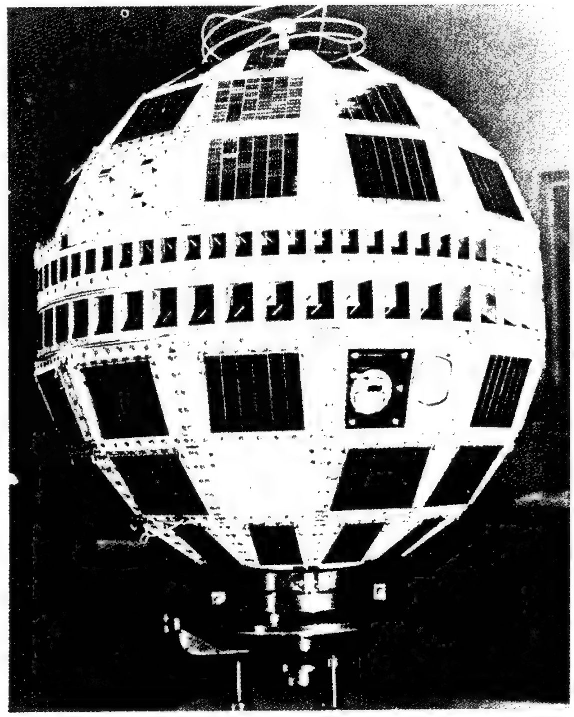

FIGURE 75-3.—Telstar spacecraft.

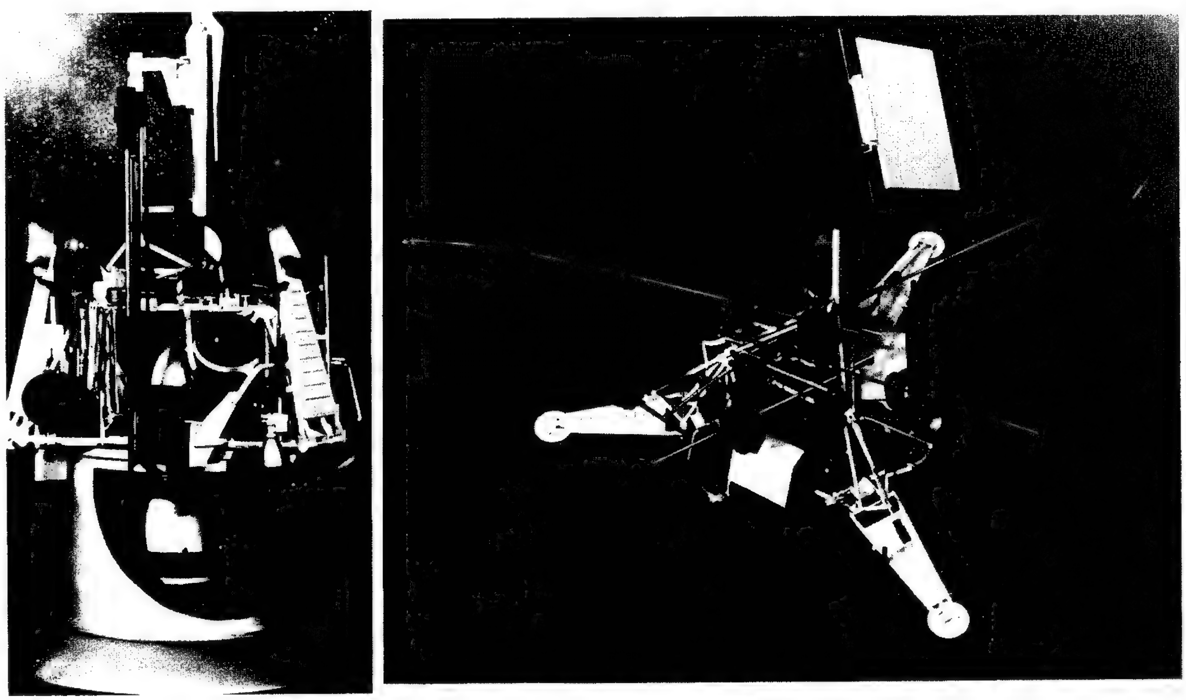

FIGURE 75-4.—Surveyor spacecraft.

that such structures are highly redundant and contain many degrees of freedom, a combination which makes dynamic analysis a difficult task.

Another good example of a deployable spacecraft is Nimbus, shown in figure 75–5. This spacecraft can be used to illustrate several key

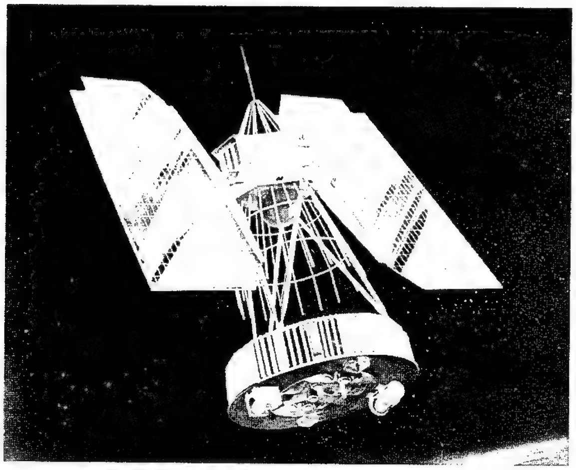

FIGURE 75-5.—Nimbus spacecraft.

structural design problems. The first of these is associated with the large solar panels which are necessary to provide the on-board power required. Whereas some spacecraft, such as those used to measure cosmic dust and radiation, may be space oriented, others designed to continually monitor a target must be oriented toward the earth or the planets. Nimbus, which is designed to photograph the earth's surface and cloud cover, is earth oriented, and consequently the solar panels are rotated relative to the remainder of the spacecraft once during each orbit in order to remain essentially perpendicular to the sun. This is necessary to maximize the absorption of solar energy by the panels. The need for panel rotations, together with the need to fold the panels for launch, introduces moving parts and associated mechanisms which inherently reduce spacecraft reliability.

Nimbus may also be used to illustrate the application of closed-cycle pneumatic shutters for temperature control of critical instrumentation components—in this case the instrumentation in the sensor ring at the base of the spacecraft. As the temperature in the compartments increases above the desired levels, the shutters open automatically and the heat is radiated to space.

Inflatable Spacecraft

Perhaps the best known example of an inflatable spacecraft is Echo I (shown in fig. 75–1). Currently NASA is in the process of developing a so-called rigidized balloon which will be 135 feet in diameter. This balloon, known as Echo A–12, is shown in figure 75–6. The skin is a soft-aluminum Mylar sandwich. The rigidization

FIGURE 75-6.—Echo A–12 (135-foot-diameter rigidized balloon).

process consists of stressing the aluminum in the shell beyond the yield point during inflation so that the wrinkles formed during the manufacturing and folding process (it is stored during launch in a spheroid having a maximum diameter of 40 inches) are permanently removed. Such techniques require careful control of the pressures involved and necessitate the use of sublimating materials such as benzoic acid.

DESIGN CONSIDERATIONS AND PROBLEM AREAS

Previous sections of this paper have presented a general discussion of some of the factors which influence the selection of spacecraft configurations and indicated some of the general problem areas. Subsequent sections are devoted to a more detailed study of problem areas and some of the design concepts which have been used or proposed for their solution. The first item to be discussed is inflation.

Inflation

During the first vertical test shot of the 135-foot balloon, it failed during the unfolding process. Subsequent analyses indicated that the rate of inflation was probably too high to allow the thin skin to carry the inertia loads imposed by the unfolded portions and the attached beacon and solar-cell modules during inflation. The analysis and associated tests also indicated that, had the balloon withstood the initial unfolding conditions, it probably would have failed during the final phase of inflation when the skin had to arrest the 6-pound beacon assembly, which would then have been traveling at a velocity estimated at about 70 feet per second.

As a result of these analyses, which involved the solution of transient stresses in a highly nonlinear membrane, and the associated tests, a system of patching reinforcements was evolved and applied to the balloon. These reinforcements, plus a reduction in the rate of inflation to achieve a final velocity of about 40 feet per second during the final phase of inflation, resulted in a spacecraft which inflated satisfactorily during the second vertical test shot.

Additional research is necessary to improve inflation techniques and to define adequately the dynamics and associated forces during the inflation process.

Lightweight Structural Components

The continued development of materials and fabrication techniques which possess high strength-to-weight ratios and can withstand the space environment is necessary to maximize spacecraft capabilities. The need for high-strength lightweight structural panels for support of solar cells is illustrated by inspection of any of the current types of spacecraft, particularly the deployable configurations such as Surveyor and Nimbus. In the construction of solar panels, for example, it is extremely desirable to have high rigidity per unit weight to provide adequate support for solar cells. As a result these structures are being constructed of honeycomb sandwiches. Although the current technology for the construction of uniform sandwich panels is good, the technology for constructing tapered panels with various joints and cutouts leaves much to be desired as evidenced by joint and bonding failures in recently constructed hardware. Both joint formation and bonding are subject to improvement by further study. As an example, the weights of adhesives in some recently constructed sandwich beams and panels constituted from 2 to 14 percent of the total weight.

In recent years, considerable attention has been given to the development of waffle-stiffened panels which are formed by chem-milling, machining, rolling, and forging processes. Figure 75–7, taken from reference 1, shows the relative weights of such structures when used as cylinders to carry bending loads. The specific-weight index is shown as a function of a structural index which is proportional to the bending moment divided by the third power of the radius. The object, of course, is to design a cylinder so that the allowable bending strength approaches the compressive yield strength. The results of the theoretical study shown in figure 75–7 indicate that the sandwich is substantially superior to the waffle as well as to other types for low values of the stress index. However, recent experimental results indicate that shells with skin-stringer stiffeners may be designed to be more competitive than indicated by the figure.

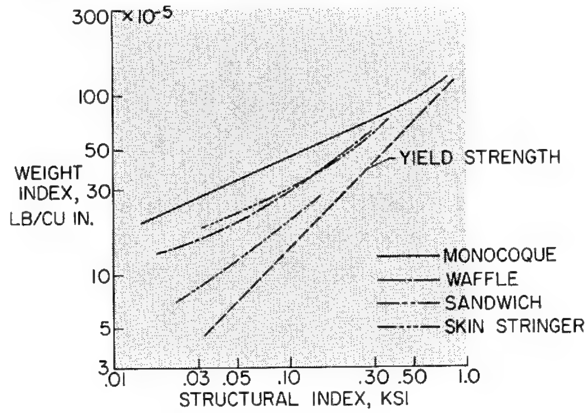

FIGURE 75–7.—Weight-strength comparisons for aluminum-alloy shells in bending.

Launch Environment

All types of spacecraft are subject to the severe shock and vibration environment imposed during the handling and launch phases.

The general problem is discussed in some detail in the literature, reference 2 for example.

The major sources of vibratory forces during launch are as follows:

Engine-ignition shocks
Pulsations of engine thrust
Turbine chugging
Rocket-engine acoustic pressures
Boundary-layer noise
Fuel sloshing
Control forces
Nonstationary aerodynamic forces
Unbalance of spinning components
Engine burnout and staging shocks

These nonstationary forces generally have a more pronounced effect on deployable spacecraft because of the fact that the effective lengths of the structural elements between supports for these vehicles are such that the natural frequencies of the spacecraft generally correspond to the high-energy input frequencies. The conditions of resonance which result lead to high-amplitude structural responses, high stresses, and excessive accelerations of the on-board scientific instruments.

An example of the complexity of the problem is shown by figure 75–8, which presents the frequency responses of a ½-scale dynamic model of the Nimbus spacecraft. The curves show the amplification factor, which is the ratio of the motion at the bottom of the paddle to the motion provided by the exciter to the base of the spacecraft, as a function of excitation frequency. The upper curve is for paddles which

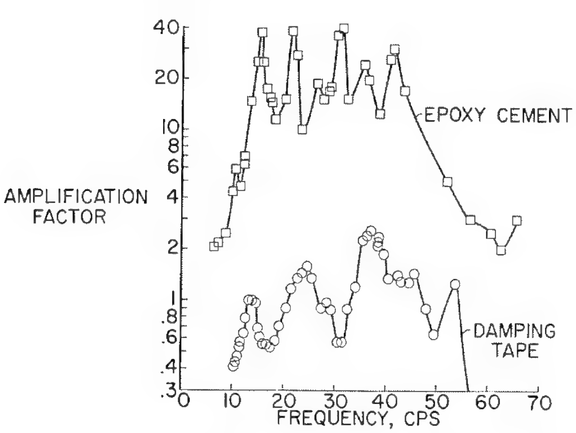

FIGURE 75–8.—Frequency response of Nimbus solar panels (½-scale dynamic model).

are formed by bonding aluminum sheets to a balsa filler by use of conventional epoxy cement. The lower curve is for the same basic type of construction except that the bonding material was replaced by a viscoelastic damping tape. The data emphasize three significant points. The first is that very high amplifications do often exist for such structures. The second is the existence of many structural resonances over a narrow frequency spectrum which extends to quite low frequencies. The third is that the response of such structures to nonstationary forces can be substantially improved by use of damping materials wherever possible.

The excitation forces are generally random functions of time with associated wide-band frequency spectrums as illustrated by the estimated sound pressure levels in the vicinity of the payload of the C–5 launch vehicle. Figure 75–9 shows the sound pressure levels outside the payload shroud as a function of frequency in octave bands. These fluctuating pressures, which result from boundary-layer buildup and flow breakdown around the shroud, have estimated peak values of approximately 157 decibels and result in an overall noise level of about 162 decibels.

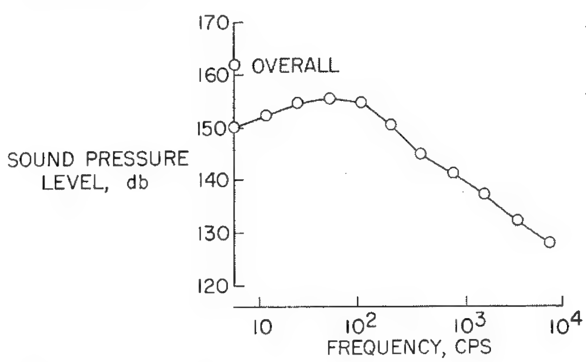

FIGURE 75–9.—Estimated aerodynamic noise pressure levels around payload of C–5 at maximum dynamic pressure.

The estimated maximum sonic-induced vibrations of a C–5 payload which would result from the acoustic pressures in figure 75–9 are shown in figure 75–10. These vibrations, which may be considered to be applied to the mounting base of the spacecraft, are of the order of 8g at frequencies above 100 cps. This is also the order of magnitude of the vibration levels imposed on spacecraft by other launch vehicles.

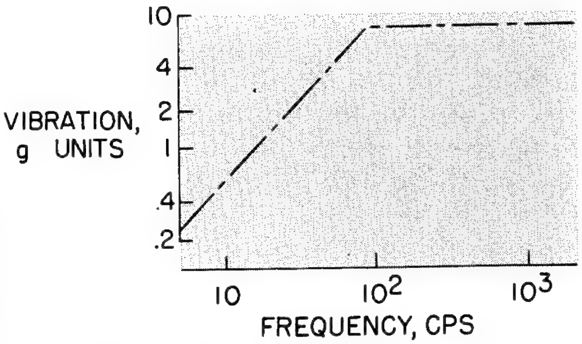

FIGURE 75–10.—Estimated maximum sonic-induced vibration around payload of C–5 at maximum dynamic pressure.

The design of a complex spacecraft to withstand the vibration environment is definitely not an easy task, but certain basic ground rules may be employed to good advantage. The first objective should be to isolate the spacecraft, or the critical components thereof, from the launch vehicle to minimize resonant responses of the spacecraft to high-frequency input motions. It is significant, in this respect, that the inputs to the spacecraft are primarily motion inputs and not force inputs.

The second objective is to introduce adequate damping into the structure by use of structural members which are inherently damped by incorporation of viscoelastic materials. Additional damping may then be applied as required by the use of discrete dampers.

The third objective, which should be started early in the spacecraft design phase, should be to determine the general dynamic or frequency response of the spacecraft by tests of simplified dynamic models, and to determine the frequencies and mode shapes of the principal natural modes. A knowledge of the mode shapes will indicate areas where distributed and concentrated damping forces may be applied to best advantage. It will also indicate nodal points where sensitive components may be installed for minimum response at critical frequencies. Dynamic-model tests have been employed to advantage for studying aircraft dynamics for many years and there is good reason to believe that they are equally applicable to spacecraft.

Several research areas which appear fruitful suggest themselves. These include the development of efficient lightweight structural materials having high fatigue resistance and structural damping, the development of analytical procedures for analysis of complex structures, and—perhaps of greatest importance—the development of highly compact and reliable instrumentation for the acquisition of in-flight vibration and acoustic environmental data.

Micrometeoroids

Any spacecraft which is designed to operate outside the earth's atmosphere for an appreciable length of time is subject to damage by micrometeoroids. The magnitude of the problem in terms of the flux and associated energies is presented by Davis in paper no. 67 of this compilation (ref. 3). During the past few years three general lines of research activity have been followed to obtain solutions to the micrometeoroid problem. The first consists of measurements of the flux by placing impact sensors on spacecraft. The second consists of the determination of the magnitude of the hazard associated with this flux by laboratory impact experiments with hypervelocity guns. The third, related to the second, consists of studies to evolve spacecraft structures which have a high probability of surviving anticipated micrometeoroid impacts.

The state of the art for solutions to the micrometeoroid problem is perhaps best illustrated by examining methods proposed recently for constructing a possible manned space station, shown in figure 75–11. This space station, in its deployed configuration shown on the left,

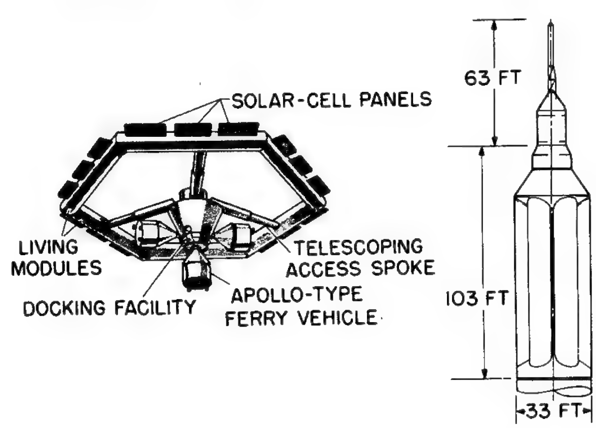

FIGURE 75–11.—Proposed manned space station. Diameter, 150 feet; area, 17,000 square feet.

has a diameter of 150 feet, an exposed area of about 17,000 square feet, and an assumed launch weight of about 170,000 pounds. (See ref. 4.) As a result of basic research studies, which show the desirability of utilizing a micrometeoroid bumper, Zender and Davidson (ref. 5) have suggested the structure shown in figure 75–12 for the tubular modules of the space station. The fundamental feature of this structure is the apportionment of basic structural materials in three layers, the outermost layer having a

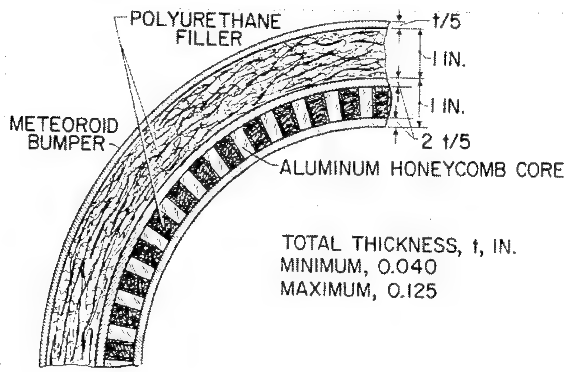

FIGURE 75–12.—Basic structure of space-station module.

thickness of t/5 and the other two layers each having a thickness of 2t/5. With this arrangement, the outer skin and filler serve as an impact bumper which breaks up the impacting body into smaller parts and effectively disperses the material over an area sufficient to reduce substantially the pointwise impact loads on the honeycomb sandwich, which is the primary load-carrying structure. The two thicknesses required are those which would yield a 50-percent probability of no penetrations per year of the entire space station according to the current low and high estimates of the flux.

The importance of developing adequate techniques for sealing micrometeoroid punctures in manned spacecraft is illustrated by figure 75–13, which shows the relative weight of the shell of the space station under discussion as a function of the probability of exceeding N punctures per year. Note that for a given probability of exceeding N punctures in a year, the weight drops sharply as the number is increased from 0 to 5. Note also that if the design is such that there is a 50-percent probability that no

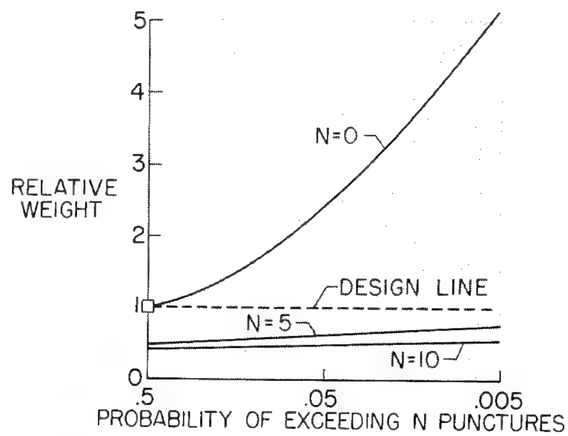

FIGURE 75–13.—Effect of allowed number of punctures per year.

punctures will occur in a year, the probability of exceeding 5 punctures per year will be very small.

Thus it appears that research in several areas needs to be continued to optimize solutions to the micrometeoroid problem. These include better definition of the flux, development of techniques for accelerating particles to micrometeoroid velocities for laboratory impact tests (current laboratory techniques yield velocities which approximate only the lower threshold of micrometeoroid velocities), and the development of reliable techniques for sealing punctures.

Life Support

A great deal of study is now being given to the establishment of the necessities for supporting man in space and to the development of necessary hardware. The basic areas of concern are summarized in reference 6. These include carbon dioxide removal, oxygen supply, water reclamation, food supply, and waste disposal. Since the problem areas are not primarily structural design, the discussion of the problem is limited here to the observation that the life support systems which meet these requirements must also endure the severe shock and vibration environments during launch.

Thermal Balance

The maintenance of spacecraft structures at approximately earth ambient temperatures during flight is currently achieved by two princi-

pal methods. The first consists of applying various types of coatings such as gold leaf, gold plate, or corrosion-resistant paints to the surface to control the ratio of the heat absorbed by the structure to the heat rejected or reradiated to space. This is the reason for the spots on the 12-foot balloon shown in figure 75–14. This balloon, known as Project Beacon, was launched into orbit to measure atmospheric density in the ionosphere.

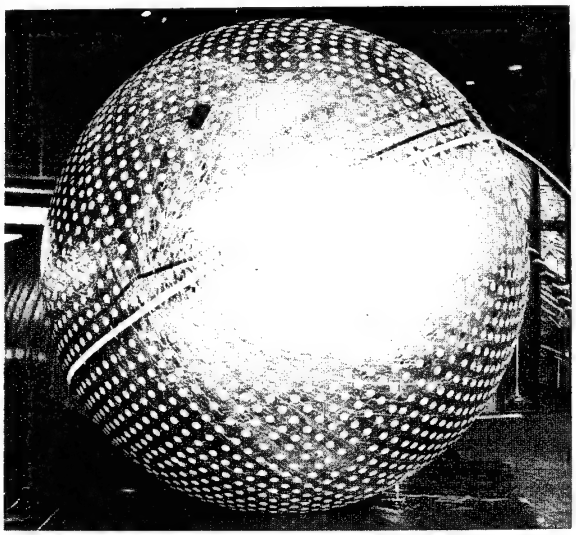

FIGURE 75–14.—Project Beacon (12-foot-diameter Mylar balloon).

The second method, which consists of providing shutters over critical temperature areas, was described in connection with Nimbus.

From the research point of view, one of the most interesting aspects of thermal control is the development of materials which become thermal radiation absorbers at low temperatures and thermal radiation reflectors at high temperatures. The coating of a reflective surface with paraffin is an example. When the temperature of the surface is below the melting point of the paraffin, the surface is opaque and absorbs radiation. However, when the paraffin melts, it becomes clear and the incident radiation passes through the film and is reflected by the subsurface. The development of better lightweight, reliable coatings or other adequate simple procedures for thermal balance is surely a matter of high priority.

Spacecraft Power Systems

There are several ways to obtain power for operation of on-board spacecraft systems. The literature (refs. 7 to 9, for example) contains summaries of the potential capabilities of various systems.

Battery systems may be considered competitive for spacecraft power requirements measured in terms of hours, and for orbital vehicles which operate while in the earth's shadow rechargeable batteries may be necessary to supply a continuous source of power. However, for spacecraft operation times measured in terms of months or years, either a means must be provided to absorb energy from solar radiation and convert it into electricity, or some form of nuclear system must be considered. The solar-cell system is the only one which is advanced to the point of being readily available. This is the reason for the dominant arrangement of solar panels on current spacecraft. A number of small solar-cell systems have been employed with good success in spacecraft, and systems having a capacity of about 500 watts are now under development.

The current state of the art in the development of spacecraft power systems may be summarized by the fact that, for an earth-orbiting spacecraft, an average of about 200 square feet and 200 pounds of solar panels are required for the generation of 1 kilowatt of power. Nickel-cadmium batteries for electrical storage average about 250 pounds per kilowatt-hour.

The lightweight concentrator concept looks promising for future long-range spacecraft such as those to go to Venus and Mars. Figure 75–15 shows five of the many types of solar collectors.

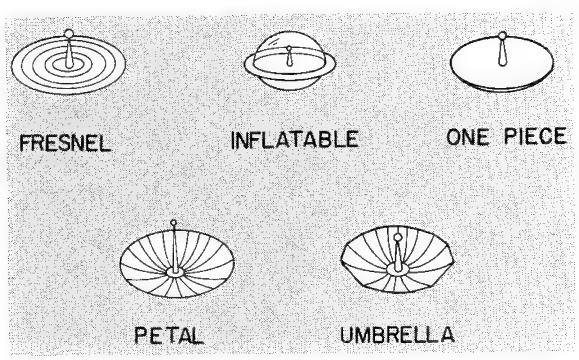

FIGURE 75–15.—Types of solar collectors.

lectors which are now being considered. All of these employ aluminum reflector surfaces and have been developed to the point where quantitative data are available to evaluate their capabilities. (See ref. 10.) Figure 75–16 shows the specific power, measured in watts per pound, for the models which have been constructed and tested to date, and the umbrella and inflatable collectors appear substantially better than other types in this respect. There are other factors such as absorber temperature, however, which are also significant.

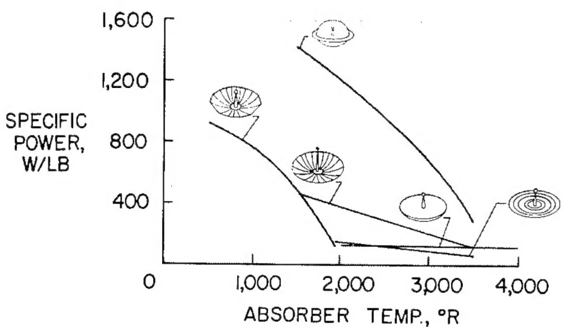

FIGURE 75–16.—Characteristics of solar collectors.

All of these collectors pose problems in packaging for launch and deployment in space to maintain the desired geometry for efficient energy absorption. Much work in this area remains to be done.

Radiation

During the past few years a great deal of study has been given to the free-space and trapped radiation which surrounds the earth. This subject is presented in some detail in reference 3. Since this is primarily a materials problem, the reader is referred to that paper for a summary of the state of the art on the subject. It should be pointed out, however, that the high weight of shielding necessary to protect man from the radiation in the Van Allen belts or from major solar-flare radiations is a difficult problem. Other means for shielding the spacecraft, such as the establishment of strong electromagnetic fields to deflect the radiation, have not progressed to the point where they appear promising. The better approach currently is to avoid the radiation belts and select flight times which correspond to minimum solar-flare activity.

Lubrication in Space Environment

Another problem area, particularly pertinent to deployable spacecraft, is lubrication. Since common lubricants which have hydrocarbon bases are highly volatile and tend to oxidize or freeze in the space environment, other types must be employed (ref. 11). In general, liquids which will stand up in space are poor lubricants.

One of the better methods of lubricating ball bearings is to encase them in a retainer ring of fiber-glass-reinforced Teflon, impregnated with molybdenum disulfide, and let them run dry. (See refs. 12 and 13.) Reference 14 presents a good summary and bibliography on the use and limitations of inorganic dry lubricants.

Another method of achieving dry lubrication consists of metal plating. Reference 14 indicates that good results have been obtained for ball bearings plated with either gold or silver in that lifetimes of several hundred hours have been achieved at vacuum levels of the order of 10^{-7} torr.

Another related problem for flights involving long exposure to the space vacuum is the possibility that the oxides and nitrides which prohibit seizure during contact of mating parts during atmospheric exposure may boil off in space and permit vacuum welding to take place. The results of studies presented in reference 15 and elsewhere indicate that this is a definite possibility and should be further investigated to assure the possibility of achieving separation of spacecraft components as required.

STERILIZATION

The NASA has a policy which requires that any spacecraft having a significant probability of encountering an extraterrestrial body be sterilized to a level of severity and length of time necessary to kill all living entities. This policy is maintained because of concern over the possibility of contaminating extraterrestrial bodies with earth life or prelife forms and the contamination of earth with extraterrestrial life forms. Although it is not expected that life will be found on the moon, there is the possibility that the scientific opportunities for study

of cosmic materials may be substantially compromised by pollution of the lunar atmosphere and surface. In the case of Mars and Venus, there is a possibility that a nutrient environment adequate for the support of biological life exists, which could result in an exponential growth of transplanted organisms. The implications of such contamination are certainly a matter of concern to United States scientists and, according to reference 16, are also of concern to Soviet scientists. Further consideration of these implications is beyond the scope of this paper; however, appropriate discussions may be found in references 17 to 19. The primary objective here is to point out the requirement for sterilization, to enumerate methods for its achievement, and to indicate some of the associated problem areas.

It may be thought that the extreme environments of flight to the moon or planets, such as ultraviolet radiation from the sun, the high vacuum of space, and the extreme temperatures and gas environments of the surface, are such that adequate sterilization is inherent. As pointed out in reference 17, such is not necessarily the case and positive steps to achieve preflight sterilization are indicated.

Procedures for sterilizing spacecraft may be summarized as follows:

(1) Heat soak at 125° C for 24 hours
(2) Expose to γ radiation at 10^7 roentgens
(3) Use liquid sterilizing additives to nonmetallic components
(4) Use surface sterilizing agents
(5) Conduct assembly operations in sterile environment
(6) Expose to mixtures of ethylene oxide and Freon-12 gases

Each of these methods suggests compromises which must be considered in the selection of spacecraft materials and techniques of fabrication and assembly.

All known living organisms are destroyed by exposure to dry steam at 160° C for 20 minutes. Since structural deficiencies of many spacecraft materials occur under these conditions, a compromise to 125° C for 24 hours is selected, which still may be too severe for many materials employed in bonding agents, seals, semiconductors, and batteries.

A second approach is to subject the spacecraft components to γ radiation dosages of 10^7 roentgens. Such radiation dosages, however, are known to be destructive to some plastics.

In the construction of spacecraft structures, it is particularly desirable to use substances such as sporicidal resins and to avoid substances of biological origin such as casein glue and shellac.

The addition of liquid sterilizing agents to nonmetallic components can be used to prevent the entrapment of live microorganisms during potting and molding processes. Similarly, liquid sterilizing agents may be used in local assembly areas such as bolt and rivet holes which may be sealed during the assembly process and therefore not be reached during the final overall sterilization process. During impact on the lunar and planetary surfaces, such areas may be exposed by structural failures which may have no destructive effects on living microorganisms.

Among the more effective and readily applied means of sterilization is the conduction of assembly operations in a sterile environment, followed by exposure to ethylene oxide and Freon-12 gas mixtures for a period of about 6 hours. After the sterilization process, the spacecraft or its components may be stored in metallic or plastic containers under continuous partial pressures to preserve sterility until launch. This technique is discussed in detail in reference 20 and the appendix of reference 19.

CONCLUDING REMARKS

Several factors which influence the design of spacecraft have been pointed out and some of the problems have been discussed. The major areas in which basic and applied research would be particularly timely and appropriate are as follows:

(1) Advanced configurations
(2) Inflation dynamics
(3) Dynamic response during launch
(4) Micrometeoroid flux and shielding requirements
(5) Thermal balance
(6) Radiation
(7) Lubrication and vacuum welding

(8) Sterilization

It should be noted that these problems include the need for additional and better facilities for simulation and study of space hazards such as radiation and micrometeoroids. Particular attention should be given to a more accurate evaluation of the natural levels of these hazards in the space environment.

REFERENCES

1. Peterson, James P.: Weight-Strength Studies of Structures Representative of Fuselage Construction. NACA TN 4114, 1957.
2. Clevenson, Sherman A., and Brooks, George W.: Considerations of Vibration Environments in Space Flight Systems. 1960 Proc. Inst. Environmental Sci., Apr. 1960, pp. 81–90.
3. Davis, Don D., Jr.: Space Environment and Its Effect on Materials. NASA-University Conference on the Science and Technology of Space Exploration, vol. 2, 1962, pp. 439–449.
4. Berglund, Rene A.: Space-Station Research Configurations. A Report on the Research and Technological Problems of Manned Rotating Spacecraft. NASA TN D–1504, 1962, pp. 9–20.
5. Zender, George W., and Davidson, John R.: Structural Requirements of Large Manned Space Stations. A Report on the Research and Technological Problems of Manned Rotating Spacecraft. NASA TN D–1504, 1962, pp. 33–44.
6. Popma, Dan C., Wilson, Charles H., and Booth, Franklin W.: Life Support Research for Manned Space Stations. A Report on the Research and Technological Problems of Manned Rotating Spacecraft. NASA TN D–1504, 1962, pp. 107–120.
7. Dawson, John R., and Heath, Atwood R.: Space-Station Power Systems. A Report on the Research and Technological Problems of Manned Rotating Spacecraft. NASA TN D–1504, 1962, pp. 59–70.
8. Zwick, Eugene B., and Zimmerman, Robert L.: Space Vehicle Power Systems. [Preprint] 867–59, American Rocket Soc., June 1959.
9. Ross, Daniel P.: Space Power Trends. [Preprint] 61–191–1885, American Rocket Soc., June 1961.
10. Heath, Atwood R., Jr.: Status of Solar Energy Collector Technology. [Preprint] 2531–62, American Rocket Soc., Sept. 1962.
11. Freundlich, Martin M., and Robertson, Arthur D.: Lubrication Problems in Space Vehicles. Preprint No. 58–53, American Astronautical Soc., Dec. 1958.
12. Anon.: Dry Film Proves Best as Space Lubricant. Machine Design, vol. 34, no. 21, Sept. 13, 1962, p. 14.
13. Van Vliet, R. M.: A Molecular Approach to Dry Film Lubrication in a Vacuum (Space) Environment. WADC Tech. Rep. 59–127, U.S. Air Force, July 1960.
14. Evans, Harold E., and Flatley, Thomas W.: Bearings for Vacuum Operation. Phase I. NASA TN D–1339, 1962.
15. Bowden, F. P., and Young, J. E.: Friction of Clean Metals and the Influence of Adsorbed Films. Proc. Roy. Soc. (London), ser. A, vol. 208, no. 1092, Sept. 7, 1951, pp. 311–325.
16. Zygielbaum, Joseph L., trans.: Soviet News Coverage of the Flight of the Second Cosmic Rocket Toward the Moon. Astronautics Information Trans. No. 10 (Contract No. NASw–6), Jet Propulsion Lab., C.I.T., Oct. 5, 1959.
17. Davies, R. W., and Comuntzis, M.: The Sterilization of Space Vehicles To Prevent Extraterrestrial Biological Contamination. Ext. Pub. No. 689 (Contract No. NASw–6), Jet Propulsion Lab., C.I.T., 1959.
18. Jacobson, N. F.: The Operations Problem of Sterilization. [Preprint] 1771–61, American Rocket Soc., Mar. 1961.
19. Posner, Jack, ed. (With appendix by Charles R. Phillips and Robert K. Hoffman): Proceedings of Meeting on Problems and Techniques Associated With the Decontamination and Sterilization of Spacecraft. NASA TN D–771, 1961.
20. Phillips, Charles R., and Hoffman, Robert K.: Sterilization of Interplanetary Vehicles. Science, vol. 132, no. 3433, Oct. 14, 1960, pp. 991–995.

☆ U.S. GOVERNMENT PRINTING OFFICE : 1963 O—672073

Publ. No.	Title	Price
SP-13	Geophysics and Astronomy in Space Exploration	.35
SP-14	Lunar and Planetary Sciences in Space Exploration	.55
SP-15	Celestial Mechanics and Space Flight Analysis	.35
SP-16	Data Acquisition from Spacecraft	.40
SP-17	Control, Guidance, and Navigation of Spacecraft	.40
SP-18	Bioastronautics	.30
SP-19	Chemical Rocket Propulsion	.40
SP-20	Nuclear Rocket Propulsion	.45
SP-21	Power for Spacecraft	.25
SP-22	Electric Propulsion for Spacecraft	.35
SP-23	Aerodynamics of Space Vehicles	.40
SP-24	Gas Dynamics in Space Exploration	.40
SP-25	Plasma Physics and Magnetohydrodynamics in Space Exploration	.50
SP-26	Laboratory Techniques in Space Environment Research	.40
SP-27	Materials for Space Operations	.35
SP-28	Structures for Space Operations	.35